LAM COKE YING

B. Sc. (Hons) Chemistry

2020

REMOVAL OF CRYSTAL VIOLET FROM AQUEOUS SOLUTION USING BANANA PEEL

LAM COKE YING

BACHELOR OF SCIENCE (HONS) CHEMISTRY

FACULTY OF SCIENCE

UNIVERSITI TUNKU ABDUL RAHMAN

OCT 2020

REMOVAL OF CRYSTAL VIOLET FROM AQUEOUS SOLUTION USING BANANA PEEL

By

LAM COKE YING

A project report submitted to the Department of Chemical Science
Faculty of Science
Universiti Tunku Abdul Rahman
Bachelor of Science (Hons) Chemistry

Oct 2020

ABSTRACT

REMOVAL OF CRYSTAL VIOLET FROM AQUEOUS SOLUTION USING BANANA PEEL

Lam Coke Ying

In this study, banana peel powder (BPP) was used as the natural and affordable adsorbent for the removal of Crystal violet (CV) in aqueous solution. BPP was characterized and analyzed with Atomic Force Microscopy (AFM), Scanning Electron Microscopy (SEM) and Fourier-Transform Infrared Spectroscopy (FT-IR). Batch adsorption conditions include biosorbent dosage, initial pH and initial dye concentration with contact time. An increase in BPP dosage facilitated percentage of CV dye removal due to availability of adsorption sites. The percentage of removal was the highest at pH 4, resulting from electrostatic attraction between cationic CV dye and anionic BPP surface. CV dye uptake by BPP was significantly higher in the early stage and achieved equilibrium at 120 minutes for all dye concentrations. The CV adsorption onto BPP followed the pseudo-second-order kinetic mechanism. Results revealed that the equilibrium data was described by Freundlich isotherm model with a correlation coefficient close to unity and a maximum adsorption capacity of

2.5763 mg/g. Properties such as abundance, effectiveness, low-cost and non-toxicity made BPP a potential biosorbent in removing CV from wastewater.

ACKNOWLEDGEMENT

First and foremost, I would like to show my sincere gratitude to my supervisor, Dr. Ong Siew Teng, for her guidance, supervision and encouragement throughout this project. I would not able to complete this project without her prompt responses and advices towards this work.

Moreover, I owe many thanks to laboratory staff for lending their precious time to help me throughout experiments. I would like to thank my course mates for their support and willingness to discuss various problems I encountered. Furthermore, I am most grateful to my family as they have always supported and inspired me.

Last but not least, I am appreciative to all researches and studies that make me having more understanding and interest on my project topic.

DECLARATION

I hereby declare that this final year project is based on my original work except for quotations and citations which have been duly acknowledged. I also declare that it has not been previously or concurrently submitted for any other degree at UTAR or other institutions.

LAM COKE YING

APPROVAL SHEET

This project entitled "**REMOVAL OF CRYSTAL VIOLET FROM AQUEOUS SOLUTION USING BANANA PEEL**" was prepared by LAM COKE YING and submitted as partial fulfilment of the requirements for the degree of Bachelor of Science (Hons) Chemistry at Universiti Tunku Abdul Rahman.

Approved by:

____

(Dr. Ong Siew Teng) Date: ________________
Assistant Professor / Supervisor
Department of Chemical Science
Faculty of Science
Universiti Tunku Abdul Rahman

FACULTY OF SCIENCE
UNIVERSITI TUNKU ABDUL RAHMAN

Date: 08 October 2020

PERMISSION SHEET

It is hereby certified that **LAM COKE YING** (ID No: **17ADB06344**) had completed this final year project entitled "REMOVAL OF CRYSTAL VIOLET FROM AQUEOUS SOLUTION USING BANANA PEEL" under the supervision of Dr. Ong Siew Teng from the Department of Chemical Science, Faculty of Science.

I hereby give permission to the University to upload the softcopy of my final year project in pdf format into the UTAR Institutional Repository, which may be made accessible to the UTAR community and public.

Yours truly,

(LAM COKE YING)

TABLE OF CONTENTS

Page

ABSTRACT **ii**
ACKNOWLEDGEMENTS **iv**
DECLARATION **v**
APPROVAL SHEET **vi**
PERMISSION SHEET **vii**
TABLE OF CONTENTS **viii**
LIST IF TABLES **xi**
LIST OF FIGURES **xii**
LIST OF ABBREVIATIONS **xiv**

CHAPTER

1 INTRODUCTION 1
- 1.1 Environmental Aspect 1
- 1.2 Dyes 2
  - 1.2.1 Crystal Violet 3
- 1.3 Biosorbents 4
  - 1.3.1 Banana Peel 5
- 1.4 Importance of Study 6
- 1.5 Problem Statement 6
- 1.6 Objectives 7
- 1.7 Scope of Study 8

2 LITERATURE REVIEW 9
- 2.1 Classes of Dyes 9
  - 2.1.1 Basic and Acid Dyes 9

2.1.2 Azo Dyes 11
2.1.3 Direct Dyes 12
2.1.4 Reactive Dyes 13
2.1.5 Vat Dyes 14
2.2 Adsorbents 16
2.2.1 Conventional and Modified Adsorbents 16
2.2,2 Biosorbents 20
2.2.2.1 Banana Peels as Adsorbents 24
2.3 Treatment of Wastewater 25
2.3.1 Adsorption 26
2.3.2 Biological Process 27
2.3.3 Coagulation-Flocculation 28
2.3.4 Ion Exchange 29
2.3.6 Membrane Filtration 30
2.4 Modelling of Kinetic and Adsoprtion Isotherm 31
2.4.1 Pseudo-First Order Kinetics 32
2.4.2 Pseudo-Second Order Kinetics 32
2.4.3 Langmuir Isotherm 33
2.4.4 Freundlich Iostherm 33

3 MATERIALS AND METHODOLOGY 34
3.1 Biosorbent Preparation 34
3.2 Adsorbate Preparation 34
3.3 Spectroscopy Analysis 35
3.4 Batch Studies 35
3.4.1 Effect of Biosorbent Dosage 36
3.4.2 Effect of Initial pH 36
3.4.2.1 Point of Zero Charge 36
3.4.3 Effect of Initial Concentration with Contact Time 37
3.4.4 Sorption Kinetics 37
3.4.5 Sorption Isotherm 38

4 RESULTS AND DISCUSSIONS 41
- 4.1 Fourier-Transform Infrared (FT-IR) Analysis 41
- 4.2 Scanning Electron Microscope (SEM) Analysis 43
- 4.3 Atomic Force Microscope (AFM) Analysis 44
- 4.4 Batch Study 45
  - 4.4.1 Effect of Biosorbent Dosage 45
  - 4.4.2 Effect of Initial pH 47
  - 4.4.3 Effect of Initial Concentration with Contact Time 50
- 4.5 Sorption Kinetics 51
- 4.6 Sorption Isotherm 53

5 CONCLUSION 56
- 5.1 Conclusion 56
- 5.2 Recommendation for Future Study 57

REFERENCES 58

APPENDICES 65

LIST OF TABLES

Table		Page
1.1	Metals in different dyes	2
2.1	Principal chemical class and application of dyes	15
2.2	List of adsorption capacity, isotherm and kinetic models based on adsorption of different dyes onto banana peels	25
4.1	Parameters of pseudo-first and pseudo second order kinetic models for CV adsorption on BPP	52
4.2	Parameters and correlation coefficients of both isotherms in CV adsorption by BPP.	55

LIST OF FIGURES

Figure		Page
1.1	Structure of Crystal Violet	4
2.1	Example of a basic dye, Carbol Fuchsin	10
2.2	Example of an acid dye, Acid Blue 25	11
2.3	Example of an azo dye, Reactive Yellow 4	12
2.4	Example of a direct dye, Direct Blue 71	13
2.5	Example of a reactive dye, Reactive Red 1	14
2.6	Redox reaction of vat dye	15
2.7	Example of a vat dye, Vat Blue 5	15
2.8	Schematic representation of Crystal Violet adsorption onto almond shell	24
2.9	Diagram of a packed column bed of adsorbent	26
2.10	Schematic representation of primary and secondary treatment	28
2.11	Coagulation-flocculation process combined with sedimentation	29
2.12	Schematic diagram of a typical demineralizer	30
2.13	Membrane filtration with incorporation of membrane bioreactor	31
4.1	FT-IR spectra of BPP	43
4.2	SEM images of raw BPP	44
4.3	AFM images of BPP	45
4.4	Effect of biosorbent dosage on CV dye removal	46
4.5	Effect of initial pH on CV dye uptake	48

4.6 Resonance structures of CV dye 49

4.7 Schematic representation of reaction between CV dye and hydroxide ion 49

4.8 Point of zero charge of BPP. 49

4.9 Effect of initial concentration on CV dye removal 50

4.10 Pseudo-first order adsorption kinetic model 51

4.11 Pseudo-second order adsorption kinetic model 52

4.12 Comparison of experimental and theoretical equilibrium concentration with contact time 53

4.13 Langmuir isotherm of CV dye adsorption by BPP 54

4.14 Freundlich isotherm of CV dye adsorption by BPP 54

LIST OF ABBREVIATIONS

AFM	Atomic Force Microscope
BP	Banana peel
BPP	Banana peel powder
BB3	Basic blue 3
BOD	Biological Oxygen Demand
BET	Brunauer, Emmett and Telle kinetic isotherm
CEN	*Casuarina equisetifolia* needle
COD	Chemical Oxygen Demand
R^2	Coefficient of determination
q_t	Concentration at time t
CR	Congo red
CV	Crystal violet
ΔpH	Difference in pH
q_e	Equilibrium concentration in mg/g
C_e	Equilibrium concentration in mg/L
exp	Experimental
$q_{e\ exp}$	Experimental concentration (mg/g) at equilibrium
n	Favorability of sorption
pH_f	Final pH
FT-IR	Fourier-Transform Infrared
K_F	Freundlich sorption constant
$\Delta G°$	Gibbs free energy

C_0	Initial concentration in mg/L
pH_i	Initial pH
$k_2q_e^2$	Initial sorption rate
K_L	Langmuir sorption constant
MG	Malachite green
λ_{max}	Maximum absorbance at a particular wavelength
q_m	Maximum monolayer sorption capacity
MB	Methylene blue
pH_{pzc}	Point of zero charge
PFO	Pseudo-first order kinetic
PSO	Pseudo-second order kinetic
k_1	Rate constant of pseudo-first order kinetic
k_2	Rate constant of pseudo-second order kinetic
RO16	Reactive orange 16
RB	Rhodamine B
R_L	Separation factor
SEM	Scanning Electron Microscope
TS	Tamarind seed
theo	Theoretical
$q_{e\ theo}$	Theoretical concentration (mg/g) at equilibrium

CHAPTER 1

INTRODUCTION

1.1 Environmental Aspect

Dyes are employed to impart colours on various materials, such as paper, textile, pulp, cosmetics and food, resulting from high stability under washing, heat and light exposure. Due to high demands in textiles currently, textile industries apply more than 1000 tons of dyes for clothing coloration. Nevertheless, the application of dyes showed a drastic growth over the past few decades. However, approximate 15 % of dyes are not properly treated and are discharged into the environment especially water streams (Vital *et al.*, 2016). Dyes become one of the significant pollutants, which are difficult to remove, as they are stable against soaps, detergents, bleaching agents and various chemicals. Besides, their complex aromatic molecular structures and antimicrobial agents used in textile dyeing make dyes to be more resist to aerobic digestion and biodegradation (Wong *et al.*, 2009; Chequar *et al.*, 2013). Purification of wastewater is now becoming a big challenge because most of the dyes are water-soluble and show acidic properties when dissolve in water (Vital *et al.*, 2016). The coloured effluent will hinder penetration of light through water and may cause disturbance towards aquatic life. In addition, some dyes are highly carcinogenic and toxic. Long-term exposure to dye solution can cause allergy, skin irritation, cyanosis and cancer (Khaled *et al.*, 2009).

Heavy metals or their ions, including aluminium, chromium, mercury and nickel, may incorporate into dyes in order to facilitate the dyeing process by their catalytic activity, or become parts of dyes as chromophores. Table 1.1 depicts the typical heavy metals found in several dyes (Shukla, 2007; Tafesse *et al.*, 2015). However, accumulation of heavy metals in textile wastewater are hazardous to living beings and environment, especially to marine lives. Therefore, pre-screening of dyes before discharging is crucial to reduce environmental pollution (Shukla, 2007).

Table 1.1: Metals in different dyes.

Types of dyes	Common metals found
Acid	Chromium, cobalt
Basic	Zinc
Direct	Copper
Mordant	Aluminium, chromium
Reactive	Lead, nickel, copper
Vat	Chromium, copper

1.2 Dyes

Coloring agents are categorized based on their capability to adsorb and reflect light at wavelength in the visible region range (400 to 700 nm). They can be further classified into two major groups, which are pigments and dyes. Pigments are mostly inorganic compounds, whereas dyes are organic compounds. Besides, pigments are larger in particle size, comparatively less soluble in water and more stable under ultra-violet exposure (Abrahart and Stothers, 2017).

Natural sources of dyes can be found everywhere. In the mid of 19th century, plants such as birch, catechu, indigo and madder were the primary sources. Dyes can also be derived from insects, such as cochineal, kermes and lac, and minerals including ferric oxide, copper carbonate and silver sulfide (Prabhu and Bhute, 2012).

Dyes are coloured compounds which able to adsorb visible light due to their conjugated system and resonance effect within structures. The presence of auxochromes in dyes, such as hydroxyl, carbonyl, and amino functional groups, enhance the stability of dyes and lead to colour changes as well. This phenomenon is termed as bathochromic shift. In addition, chromophores are responsible for the colour by incorporated themselves in the conjugated system of dyes. The examples of chromophores are C=C double bond, quinoid ring, azo, carbonyl, nitro and thiol groups (Carreon-Valencia *et al*., 2008).

1.2.1 Crystal Violet

Molecular formula and molar mass of Crystal Violet (CV) are $C_{25}H_{30}N_3Cl$ and 407.979 g/mol, respectively. It is a cationic triarylmethane dye, also known as Methyl Violet or Gentian Violet. Condensation of dimethylaniline and formaldehyde gives a colourless leuco dye molecule. The leuco dye is then oxidized into purple coloured cationic CV dye (Thomas and Udo, 2000). It is mostly used in textile dyeing, biological staining, printing and paint manufacturing. Besides, CV can also be employed as antimicrobial agent, antiseptic and disinfectant. However, CV is carcinogenic and non-biodegradable. Exposure to CV continuously causes skin and eye irritation, cornea injury, respiratory allergy and kidney failures (Ahmad, 2009; Chakraborty *et al*., 2011)

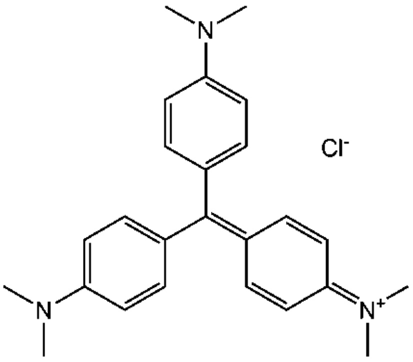

Figure 1.1: Structure of Crystal Violet.

1.3 Biosorbents

In recent decades, scientists have pay more attentions on various biological materials, including agricultural waste and bacteria, for dye removal due to their high effectiveness, low capital requirement, biodegradability and abundance. Biosorbents contains several functional groups in their structures such as amino, carboxyl, thiol, sulphydryl and hydroxyl groups. These groups act as the adsorption sites for adhesion of dye molecules onto biosorbent surface. Besides, the purpose of pre-treatment and modification of biosorbents is to boost their adsorption ability as efficient as the conventional adsorbents (Wang and Chen, 2009). For instance, phenol group is incorporated into lignin to enhance its biosorption ability. Adsorption processes involving biosorbents offer numerous benefits such as low cost, simple operation, improve efficiency, high selectivity, short operation duration and minimal generation of hazardous wastes (Inoue *et al*., 2017).

1.3.1 Banana Peel

In term of botanical, banana belongs to Musaceae family and is native to Africa, Asia and Australia. It is one of the major fruits consumed in the world. In 2018, production of bananas in Malaysia was about 375000 tones (Knoema, 2018). Out of 100 kg of banana plants, other parts of plants like leaves, pseudo-stem, fruits and rachis contribute for about 15 kg, 50 kg, 33 kg and 2 kg respectively (Pishgar *et al*., 2013). The peel consists various functional groups such as amine, hydroxyl and carbonyl groups, which responsible for adsorbate binding. Besides, 60 % of carbohydrate content found in banana peels may lead to microbial growth (Deshmukh *et al*., 2017). Hence, banana peels are dumped from market and household areas as agriculture wastes for most of the time.

1.4 Importance of Study

This study evaluates the adsorption ability of banana peel on removal of CV dye from aqueous solution. The results obtained from batch experiments will directly determine the effectiveness of banana peel as a biosorbent. It also serves as an evidence or suggestion for future research on wastewater treatment. Modification can be made in order to produce and utilize banana peel biosorbent in large-scale dye removal treatment. In addition, application of the banana peel lowers the economic burden of textile industries, as well as reduces the risk of environmental pollution.

1.5 Problem Statement

The drastic increase of trending in fabrics had resulted to the upsurges in generation of dye-containing wastewater and environmental pollution cases. About 100 billion of clothing are produced globally each year and the textile production rate shows a two-fold increase starting from 2000 to 2014 (Nadiah, 2018). However, poor compliance of textile industries to environmental regulations due to cost considerations, limited treatment technology, lack of green industry practices and insufficient resources. For example, small- and medium-scaled textile industries discharge effluent into surroundings illegally due to lack of investment in treatment and equipment (Sharifuddin and Ang, 2017). In the case of *batik* making in Malaysia, wastewater is often coloured and contains vast arrays of organic pollutants. Effluents with high Chemical

Oxygen Demand, COD value are the major causes of water pollution in Malaysia (Yaacob *et al*., 2015).

Conventional effluent treatments, including membrane filtration, electrochemical process and ion exchange technique, are efficient and effective, but they require high cost, special handling, complex operation and high energy consumption. Meanwhile, usage of synthetic or modified adsorbents such as activated carbon and nanofibers is also a burden to smaller sized industries for dye removal due to high capital requirement. Therefore, development and implementation of biosorbents for wastewater treatment is necessary recently by taking into accounts their adsorption capability, cost requirement, operation simplicity and toxicity.

1.6 Objectives

The goals of this study are:

1. To prepare a low cost and effective biosorbent from banana peel for CV dye removal from aqueous solution.
2. To characterize and analyze the structure, morphology and topography of the biosorbent using FT-IR, SEM and AFM.
3. To study the parameters affecting the dye adsorption using biosorbent under batch experiment conditions.

4. To determine the kinetic mechanism and sorption isotherm of dye adsorption.

1.7 Scope of Study

This study emphasizes the adsorption capacity of raw banana peel (BP) as a biosorbent, characterization of banana peel surface and adsorption behaviors of the biosorbent. BP was employed due to availability, low-cost and biodegradability. Crystal Violet dye was selected as it is considered as carcinogenic and biohazardous dye. Three parameters were studied, including amount of biosorbent used, initial dye concentration with contact time and initial pH of dye solution.

CHAPTER 2

LITERATURE REVIEW

2.1 Classes of Dyes

2.1.1 Basic and Acid Dyes

The first synthetic dye discovered by William Henry Perkin in 1856 is Mauveine, a basic dye consisting aromatic rings in which different amount of methyl groups were substituted in different arrangements (Scaccia *et al.*, 1998). Basic dyes are termed as cationic dyes because the chromophores present in the structures carry positively charge in aqueous solution. Typical functional groups of basic dyes are $–NR_3^+$ and $=NR_2^+$. Most of them are water soluble with poor light and washing fastness. Basic dyes are commonly employed onto paper, nylon, silk, cotton and polyesters when the shade brightness is prior to fastness properties. Reaction of triarylmethane found in basic dye is similar to Lewis acid as its sp^2 hybridized carbon atom can accept electrons from hydroxyl group, forming carbinol base, which can be used as a pH indicator. Besides, basic azine dyes are synthesized via subsequent oxidation processes. Currently, sulfonated azine dyes are still widely used in society. For example, Nigrosine Spirit Soluble is applied in leather shoes polish (Hunger, 2003).

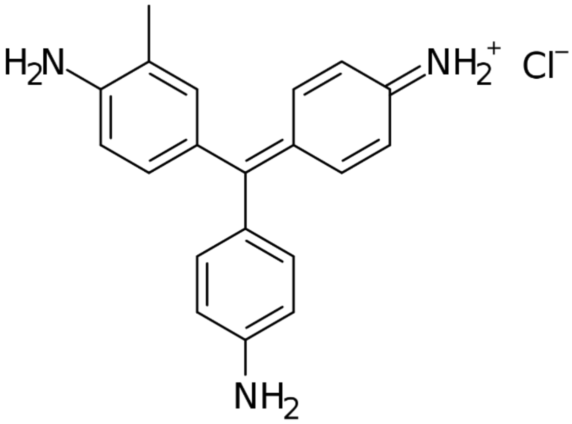

Figure 2.1: Example of a basic dye, Carbol Fuchsin.

As for acid dyes, they are bearing negatively charged of O^-, SO_3^- and COO^- as chromophores in their structures. Similar to basic dyes, acid dyes are soluble in aqueous solution and widely used in dyeing of wool, leather, paper and acrylics (Hunger, 2003). They are comparatively better than basic dyes in fastness properties and provide pure colours. Acid dyes can be further categorized based on their structures into anthraquinone-, azo-, and triarylmethane-based dyes. In term of dyeing methods, they are classified into levelling acid, milling and metal complex acid dyes. Levelling acid dyes require acid baths, in cooperation with levelling agents, such as linear ester (Weckler *et al*., 1981), diary ether (Kuehni *et al*., 1982) and sodium hydroxysulfonate compounds (Ohba *et al*., 1990) to facilitate migration of dye molecules towards textile without extreme dye consumption. Conversely, acid bath is not necessary for milling dyes. They are heavier compared to the former dyes and travel slower towards fabric. Lastly, metal complex acid dyes are made by complexation with metal ion which results to the highest washing fastness among the three dyes. They are often employed on nylon and polyamide fibres (Richards, 2012).

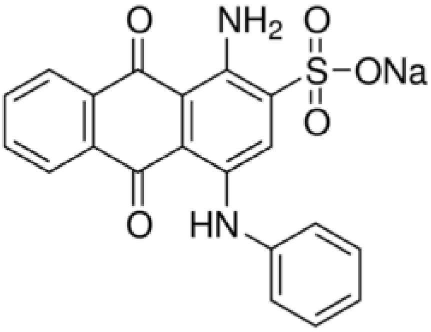

Figure 2.2: Example of an acid dye, Acid Blue 25.

2.1.2 Azo Dyes

Name of azo dyes comes from the presence of azo group (–N=N–) as functional groups. They are synthesized via azo coupling in which a coupling compound, or called as napthol, reacts with an azo-containing component. Application of azo dyes in dyeing industries is popular due to low cost, obvious colour shades, excellent perspiration and bleaching fastness (Mahapatra, 2016). On the other hand, monoazo dyes bearing heterocyclic coupling compound such as pyrazolone are mostly yellow in colour, while diazo dyes comprise multiple aromatic rings and substituted aniline or sulfonated aminonaphthalene (Hunger, 2003).

Azo dyes can be either anionic or cationic dyes, based on the charge carried by chromophores. For anionic azo dyes, at least one sulfonic acid is found and involves in dyeing process. On the other hand, presence of amino groups results to formation of cationic azo dyes. They are mostly used with mordant dye in cotton dyeing, but less contribution in paper and plastics dyeing. Both types of azo dyes can be served as substantive dyes as they exhibit remarkably affinity towards polymeric fibres (Carreon-Valencia *et al*., 2008).

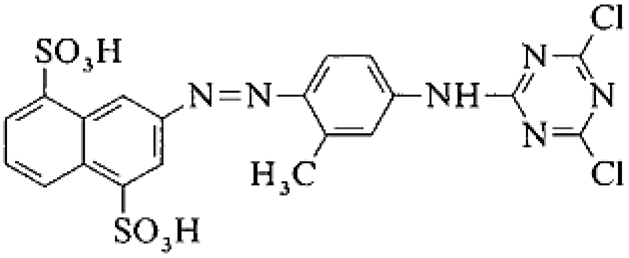

Figure 2.3: Example of an azo dye, Reactive Yellow 4.

2.1.3 Direct Dyes

Direct dyes or substantive dyes apply directly from aqueous solution onto textile, especially cellulosic fibres, by weak hydrogen bonds and Van der Waals interaction. Majority of direct dyes are soluble in water due to presence of sulfonic acid functional groups, but they experience a decrease in solubility with increasing in molecular weight. However, sequestering agents are introduced into dyebath to remove calcium and magnesium from hard water. These metals form scums when they are in contact with certain direct dyes. Although the colours of direct dyes are not as vivid as basic dyes, but they exhibit better light and washing fastness. Post treatments such as metallic complexing and diazotization enhance the fastness properties and colour brightness. In addition, most of direct dyes consist azo groups, together with other chromophores such as stilbenes, thiazoles and oxazines. The benefits of direct dye application include simple dyeing operation, low cost, as well as good solubility in water (Mahapatra, 2016).

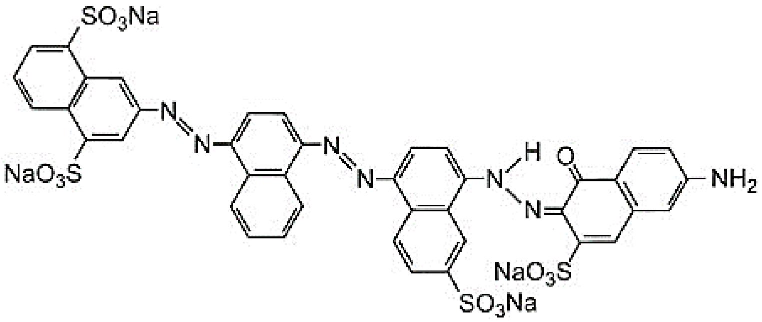

Figure 2.4: Example of a direct dye, Direct Blue 71.

2.1.4 Reactive Dyes

Direct, vat, and azo dyes were often used for cellulosic fibres before the introduction of reactive dyes in dyeing industries. The dyeing process involves covalent bonding between hydroxyl groups of fibre and reactive groups of dye. The reactive group is commonly a heterocyclic ring bonded to chromophore by a bridging group. Reactivity and properties of dyes are enhanced by substituents such as chlorotrazinyl and vinylsulphone of heterocyclic rings. In addition, incorporation of solubilizing group results to greater dye solubility in aqueous dyebath. Reactive dyes are extensively employed nowadays because of simple dyeing operation and bright colour shading. Moreover, they exhibit excellent washing fastness due to firmly adhesion of dye molecules onto fibres with the aid of basic reagent added in dyebath. The unreacted dyes are rinsed off from fibres using hot water (Matyjas and Rybicki, 2003).

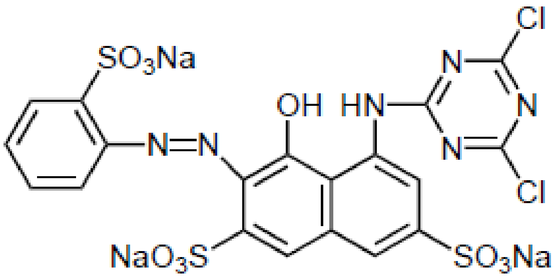

Figure 2.5: Example of a reactive dye, Reactive Red 1.

2.1.5 Vat Dyes

In 19th century, indigo was extracted from plants and dissolved in wooden vats. After biological fermentation, natural vat dyes were produced and applied in cotton dyeing. Neutral form of indigo is an insoluble purplish-blue pigment and it turns to yellowish-green soluble form when reduction takes place. Once after cotton adsorbed the dye and exposed to air, the indigo undergoes oxidation and converts back to purple colour. Alkaline acts as reducing agents in dyebath to dissolve vat dyes, which will be adsorbed by cellulosic fibres. Oxidizing agents such as hydrogen peroxide and boric acid may leads to over-oxidation of some vat dyes. It causes vat dyes to retain as insoluble form, instead of soluble dyes. Atmospheric oxygen is an appropriate oxidizing agent for redox reaction of vat dyes, but longer operation time is needed. Besides, most vat dyes consist of carbonyl groups, which undergo delocalization with conjugated ring system during redox reaction. It facilitates the interaction of dye and hydroxyl group (Aspland, 1992).

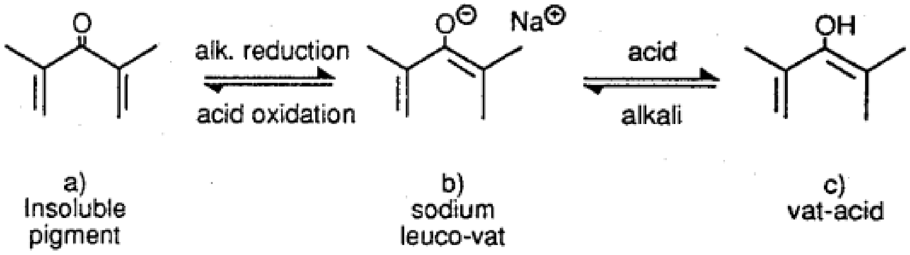

Figure 2.6: Redox reaction of vat dye.

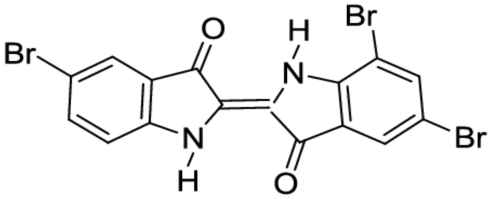

Figure 2.7: Example of a vat dye, Vat Blue 5.

Table 2.1: Principal chemical class and application of dyes.

Types of dyes	Principal chemical class	Substrate materials
Acid	Azo, anthraquinone, triarylmethane, nitro, nitroso	Cotton, nylon, silk, paper, leather
Basic	Azo, diarylmethane, triarylmethane, oxaanthracene, oxazine, thiazine	Paper, polyester, polyamide, inks, nylon
Direct	Azo, oxanine	Rayon, cotton, nylon, leather
Reactive	Azo , anthraquinone, formazan, oxanine	Wool, silk, cotton
Vat	Anthraquinone, indigoid	Rayon, cotton

2.2 Adsorbents

An adsorbent is the species that provide its surface for attachment and aggregation of adsorbates. Vast arrays of studies had been done on effectiveness of adsorbents removing dye from aqueous solution. An excellent adsorbent should have heterogeneous surface with uniform pores distribution, which leads to an increase in surface area exposed to adsorbates. Meanwhile, the adsorption process is enhanced with greater pores volume present (Dutta *et al*., 2011; Hussin *et al.*, 2015). Besides, capital requirement, abundance, stability and disposal treatment are some of consideration factors when using an adsorbent.

2.2.1 Conventional and Modified adsorbents

Based on the study by Zhou *et al*. (2018), shrimp shell was treated with sodium hydroxide and hydrogen peroxide in order to decolourize and remove protein. Lower organic materials led to smaller particle size of treated shrimp shell. As a result, the surface area of treated shrimp shell particles was comparatively larger than that of natural shrimp shell. Besides, SEM images showed that the modified adsorbent had greater pore volume for Congo Red dye adhesion. Generally, dye uptake was enhanced with greater initial concentration and lower initial pH of dye solution. The adsorption capacities of modified and untreated adsorbents were 288.2 mg/g and 256.4 mg/g, respectively. Both of the adsorbents were more effective than chitin. Pseudo-second order kinetic rate and Langmuir isotherm well described the adsorption behavior of shrimp shell.

Dye adsorption capability of inorganic silica was studied by Krysztafkiewicz *et al*. in 2002. Silica adsorbent was modified using two types of amino silane coupling agents to substitute silanol groups present on adsorbent surface with amino groups. Water-adsorbent interaction was minimized, at the same time, adsorption ability of modified silica adsorbent was improved. Four different dyes were employed, which are Reactive Blue 19, Acid Violet 1, Acid Red 18 and Acid Green 16. Regardless of the types of coupling agents, dye adsorption increased with greater amount and surface area of adsorbent. The highest dye uptake was 99.8 % using 10.0 parts by weight of silica modified with N-2-(aminoethyl)-3-aminopropyltrimethoxysilane in Acid Violet 1 dye solution.

According to Tahir *et al*. (2010), montmorillonite clay, a mineral crystal, can be used to remove Malachite Green and Fast Green dyes from aqueous solution. Untreated montmorillonite clay had high affinity towards anionic Fast Green dye, whereas acid-treated clay showed higher adsorption of cationic dye, Malachite Green. The percent removal increased with higher initial concentration, agitation time and temperature. The highest removal of both dyes was around 97 %. Besides, experimental data fitted well in Langmuir isotherm and the values of separation factor, R_L were in between 0 to 1 under different temperatures (303 to 318 K). Gibbs free energy, $\Delta G°$ of adsorption gave negative values for all system temperature as well.

Namasivayam and Kavitha (2002) prepared activated carbon from coir pith and studied its sorption ability towards Congo Red. The dried coir piths were grinded into powder and carbonized. Based on the results, the dye adsorption increased with increases in agitation time, initial concentration and amount of adsorbent used. The percent dye removal was the highest at pH 2 due to electrostatic attraction between negatively charged Congo Red and protonated carbon of adsorbent. The results were well described by both Langmuir and Freundlich isotherms. The adsorption behavior followed pseudo-second order kinetic law with adsorption capacity of 6.72 mg/g.

The research carried out by Yang *et al*. (2011) found that surfactant-modified *Aspergillus oryzae* (a fungus) had better sorption ability towards Acid Blue 25 and Acid Red 337 in binary system than untreated adsorbent. Introduction of surfactant to *Aspergillus oryzae* resulted to high surface porosity and additional C-N vibration band in FT-IR spectrum, which acted as one of the adsorption sites. Furthermore, researchers also found that the two dyes in binary system competed for available adsorption sites. Comparatively, the competition was greater using unmodified adsorbent. It further indicated that there were more adsorption sites on surface of surfactant-modified fungus. However, both adsorbents showed better adsorption to Acid Blue 25 in binary system. The adsorption process obeyed to the extended Langmuir isotherm model.

According to Hussin *et al*. (2015), adsorption efficiency of durian leaf was improved by incorporating carboxylate groups via alkaline treatment.

Based on the experimental SEM analysis, the surface of treated durian leaf became more porous compared to that of natural durian leaf. In the study, it showed that Methylene Blue uptake by modified adsorbent increased with initial dye concentration and contact time as well. The optimum amount of adsorbent and pH for maximum adsorption were 0.04 g and pH value higher than 4, respectively. The results followed pseudo-second order kinetic model and Langmuir isotherm with a maximum adsorption capacity of 125 mg/g.

Adsorptive removal of Basic Blue 3 (BB3) and Reactive Orange 16 (RO16) using both natural and quaternized sugar cane bagasse was investigated by Wong *et al*. (2009). The raw sugar cane bagasse was pre-treated with sodium hydroxide, followed by quaternary ammonium chloride to introduce quaternary nitrogen cation to the structure. Results showed that the percent removal of anionic RO16 by quaternized adsorbent was much higher than that by raw adsorbent. It was due to electrostatic attraction between the cationic quaternary nitrogen and negatively charged RO16. However, adsorption of cationic BB3 onto modified sugar cane bagasse was lower than using raw one due to repulsive forces between positively charged adsorbent surface and cationic dye. The experimental data for both adsorbents fitted well in Langmuir and Freundlich isotherms. The mechanism of adsorption followed pseudo-second order kinetic model.

2.2.2 Biosorbents

In 2015, Tanzim and Abedin used pomelo peels in the investigation of Methylene Blue (MB) removal form aqueous solution. They stated that application of conventional adsorbents were costly, including activated carbon, clay minerals and zeolites. Hence, the usage of biosorbent is emphasized nowadays. In the study, optimum MB adsorption conditions were using 1 g of pomelo peel powder in 150 ml of 100 ppm dye solution with initial dye pH of 5. The dye removal achieved 95 % after 90 minutes. Langmuir isotherm was the best modelling for the result data with adsorption capability of 28.57 mg/g.

Casuarina equisetifolia needle (CEN) was employed by Kooh *et al*., (2015) to remove Rhodamine B (RB) dye from aqueous solution by adsorption. The experimental SEM images showed that the surface of biosorbent was heterogeneous with countless pores, which increased surface area and facilitated dye adsorption. Meanwhile, shifting of O-H, N-H and C-H vibration bands observed in FT-IR spectra indicated that these functional groups of CEN participated in RB removal. The adsorption process obeyed to the pseudo-second order kinetic and Langmuir isotherm model. The adsorption capability of CEN was 82.3 mg/g. In addition, hydrophobic interaction was dominant prior to electrostatic attraction with the presence of salt. Therefore, researchers suggested that CEN was an appropriate biosorbent to treat effluent with high ionic strength.

Researcher Ofomaja (2007) carried out the study based on sorption kinetics and isotherms involving palm kernel fibre and Methylene Blue dye. After 60 minutes, it was found that maximum percent dye removal and equilibrium sorption improved from 95.65 % to 99.15 % and 217.95 mg/g to 223.41 mg/g, respectively when system temperature increased from 299 K to 339 K. These were due to greater mobility of MB and higher reactivity of functional groups present on biosorbent surface under higher temperature condition. The Gibbs free energy gave negative values for all temperature-system, which indicated that the adsorption process was spontaneous. Besides, the experimental data could be explained using Langmuir isotherm and pseudo-second order kinetic model.

According to Sumalapao *et al*. (2016), calamansi (*Citrus microcarpa*) peels is a possible biosorbent to be used in Congo Red (CR) dye removal. Similar to other biosorbents, calamansi peel exhibited greater adsorption with increase in contact time and amount of biosorbent added. The adsorption behavior was well described by intraparticle diffusion kinetic model with smaller relative error and higher coefficient of determination compared to those of pseudo-first order, pseudo-second order, Elovich and MacArthur-Wilson models. A large number of adsorption sites results in improvement of boundary layer effect and hence, faster intraparticle diffusion process. The maximum adsorption capacity was 2.205 mg/g.

Tahir *et al*. (2008) utilized *Ulva lactuca*, *Sargassum* (both were algae) and alumina to investigate the adsorption behavior for Methylene Blue (MB) dye removal. It proved that the dye removal by biosorbent achieved more than 80 % at 303 K to 318 K, which possessed similar effectiveness as conventional alumina adsorbent. Furthermore, Gibbs free energy values of both biosorption were relatively more negative than that of alumina-system adsorption. Researchers suggested that the adsorption using *Ulva lactuca* and *Sargassum* was thermodynamically more favorable than using alumina in MB removal. Besides, three adsorbent systems followed both Langmuir and Freundlich isotherms.

In term of sorption modeling and kinetic studies, adsorption behavior of *Cocos nucifera*, coconut bunch waste was investigated by Hameed *et al*. (2008). Based on experimental FT-IR spectra, shifting and disappearing of some vibration bands such as carboxyl and amino functional groups were observed. It was due to their involvement as adsorption sites for basic Methylene Blue dye to adhere. SEM images also showed that the porous biosorbent surface became more evenly after dye uptake. In addition, the biosorbent performed better under alkaline condition and higher initial dye concentration. Adsorption equilibrium was established within 3 to 5 hours. The result data was best described by pseudo-second order model and Langmuir isotherm with adsorption capacity of 70.92 mg/g.

Rajeshkannan *et al.* (2011) suggested that the optimum condition of Malachite Green (MG) dye adsorption by tamarind seed (TS) were adding 2.85 g of biosorbent (particle size of 0.17 mm) into 100 mg/L of dye solution and agitating at 2090 rpm for 202 minutes. The dye solution and system temperature shall be maintained at pH 7 and 37 ℃, respectively. Based on the results, Langmuir isotherm and pseudo-first order kinetics showed better values of coefficient of determination. The adsorption capacity was found to be 54.95 mg/g. According to FT-IR spectrum of TS, hydroxyl, carboxyl, sulfonic and amine peaks were observed and expected to be active adsorption sites.

Based on Loulidi *et al*. (2020), percent removal of Crystal Violet (CV) dye by almond shell powder was up to 82 % under alkaline condition at 20 ℃. At the same time, dye uptake increased with greater biosorbent dosage and contact time. Equilibrium was reached at 90 minutes. Langmuir isotherm and pseudo-second order kinetic model were appropriate to describe the results obtained. The adsorption capacity of unmodified almond shell was 12.2 mg/g. Moreover, researchers suggested that CV dye was adsorbed onto biosorbent surface by hydrogen bonding between nitrogen atom of CV with hydroxyl group of biosorbent.

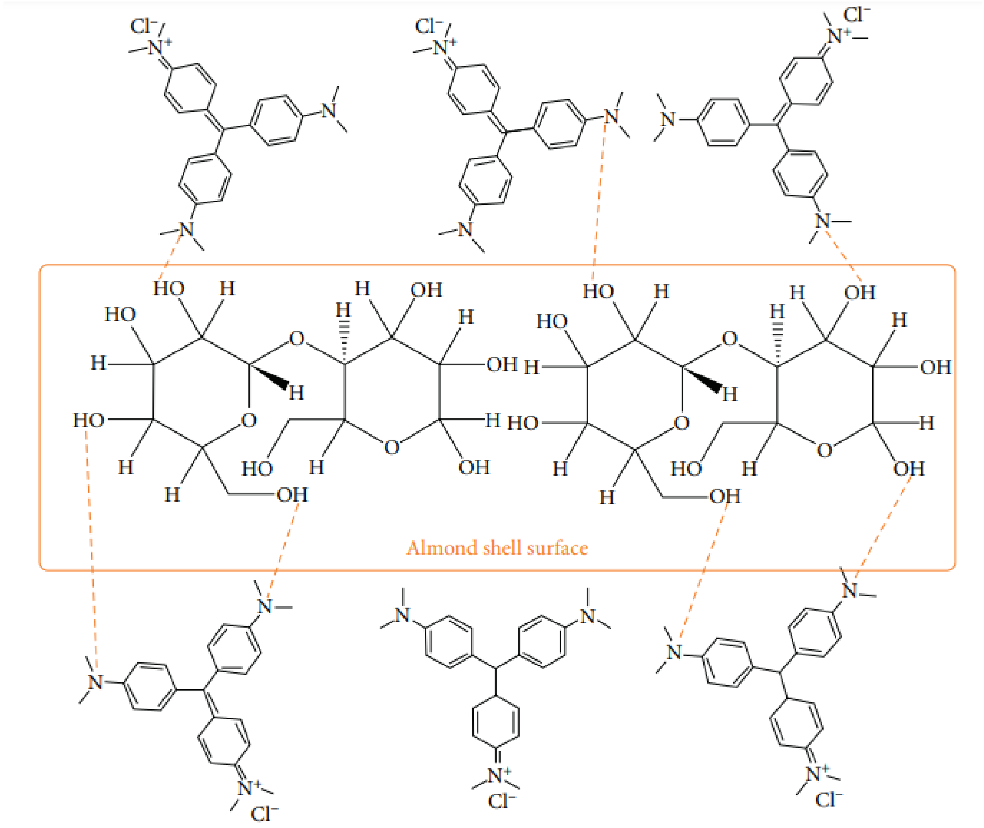

Figure 2.8: Schematic representation of Crystal Violet adsorption onto almond shell.

2.2.2.1 Banana Peels in Dye Removal

Numerous studies on adsorption capability of banana peel (BP) had be done previously. Researchers suggested that BP was a potential biosorbent in dye removal from aqueous solution due to low-cost, high sorption ability, biodegradability and high effectiveness at nearly neutral dye solution. The tolerable pH of textile wastewater is within the range of 5 to 9 (Pollution Control Department, 2017). By adjusting the pH of dye effluent, it is expected that BP can exhibit maximum dye adsorption.

Table 2.2: List of adsorption capacity, isotherm and kinetic models based on adsorption of different dyes onto banana peels.

Dye applied	Adsorption capacity (mg/g)	Isotherm	Kinetic model	Reference
Basic Blue 159	-	Langmuir	2nd	Pishgar *et al.*, 2013
Orange G	20.9	Freundlich	2nd	Stavrinou *et al.*, 2018
Methylene Blue	211.9	Langmuir	2nd	Stavrinou *et al.*, 2018
Methylene Blue	120	-	-	Dahiru *et al.*, 2018
Methylene Blue	18.65	Langmuir	2nd	Amel *et al.*, 2012
Malachite Green	107	-	-	Dahiru *et al.*, 2018
Malachite Green	243.90	Freundlich	2nd	Saechiam and Sripongun, 2019
Rhodamine B	13.20	Freundlich	-	Annadurai *et al.*, 2002
Amido Black 10B	7.90	Freundlich	-	Annadurai *et al.*, 2002
Reactive Red	11.68	Redlich-Peterson	2nd	Kamar *et al.*, 2018
Reactive Black 5	211.80	Langmuir	2nd	Munagapati *et al.*, 2019
Congo Red	1.73	Langmuir	2nd	Mondal and Kar, 2018

*2nd: Pseudo-second order kinetic

2.3 Treatment of Wastewater

A variety of methods including physical, chemical and biological were developed in order to remove dye from effluent, for instance, membrane filtration, coagulation, electrochemical reaction and much more. However, every method has its own superb application and limitation. Some methods are highly efficiency for dye decolourization, but thermodynamically unfavorable.

2.3.1 Adsorption

Adsorption is effective, economical, readily available, easy to operate and yet environment friendly as various kinds of biosorbents from agriculture waste can be used. Adsorption is a surface phenomenon in which atoms, ions or molecules, so called adsorbates, adhere and accumulate on the surface of a substance. As a result, they aggregate and form a thin layer onto the surface of adsorbent. For instance, a cylindrical reactor was filled with adsorbents in a packed column bed. It is frequently employed nowadays as it is effective with great productivity and high operational simplicity. By changing the types of adsorbents, various compounds can be removed from effluent (Papirio, 2017).

However, limitation of adsorption process such as sludge generation, time-consuming and ineffective of particular adsorbent are the challenges in wastewater treatment industries.

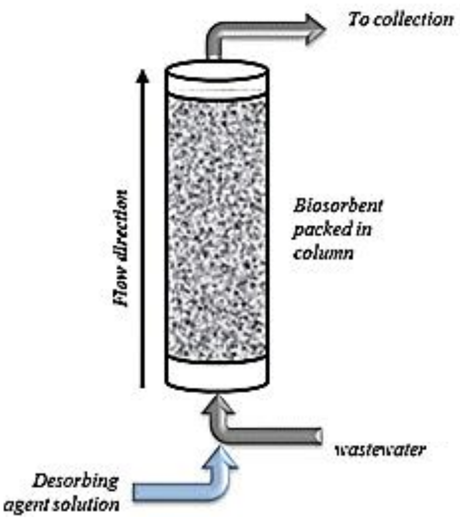

Figure 2.9: Diagram of a packed column bed of adsorbent (Papirio, 2017).

2.3.2 Biological Process

Biological-based methods, termed as secondary methods, emphasize degradation of soluble organic compounds using green materials and reagents such as microorganism after removing solid impurities in primary treatment. Excellent benefits of applying this method in industries are environmental friendly, low capital requirement and less sludge production. Moreover, most dyes can be degraded into a species with lower toxicity (Bhatia *et al.*, 2017). There are three common biological-based techniques which are trickling filtration, activated sludge treatment and oxidation reaction. Among these techniques, application of activated sludge is the most popular. Microorganisms degrade the organic compounds in aeration tank and the sludge generated is passed to secondary clarifier for settling down. Treated effluent is skimmed from clarifier for further disinfection, whereas the sludge will be discharged (Nathanson and Ambulkar, 2010).

However, biological process is ineffective in dye decolourization and treatment of wastewater with high concentration of Biological Oxygen Demand (BOD). In addition, solid particles cannot be processed via this method, thus, an external treatment of solid removal is required. The major factors influencing biological process in dye removal are temperature, amount of dissolved oxygen and pH of system. The operation condition must be strictly controlled and maintained (Samer, 2015).

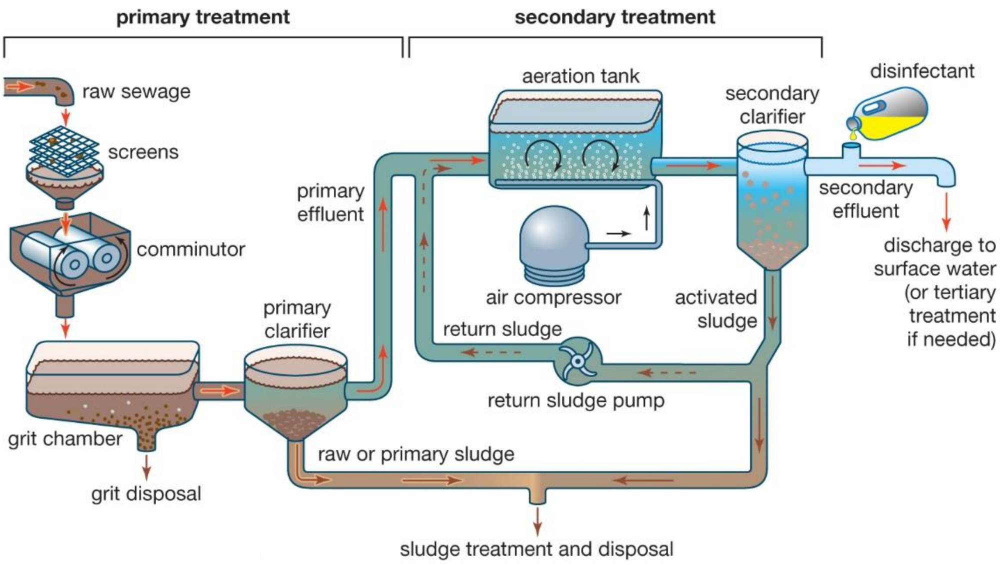

Figure 2.10: Schematic representation of primary and secondary treatment (Nathanson and Ambulkar, 2010).

2.3.3 Coagulation-Flocculation

Coagulation–flocculation in wastewater treatment is carried out with combination of sedimentation and filtration. This physical method is typically useful in removal of sulphur and disperse dye. First of all, coagulant will be introduced into effluent to destabilize dye molecules by neutralizing the electrical charge of dyes. As a result, suspension solution will be formed as coagulant entraps the dye molecules in effluent. Then, polymers are added with stirring to aggregate the relatively small suspended particles into larger flocs for easy separation. After settling down or sedimentation, the flocs are filtered away from aqueous solution.

However, this method exhibits low effectiveness in removal of acid, direct, reactive and vat dyes. Sludge may be produced during effluent treatment which acquire high cost to handle and process. Furthermore, dye decolourization performance is not as excellent as other methods. The pH of the effluent must be controlled and adjusted to neutral pH as coagulation reaction is highly sensitive to pH changes (Redah, 2016).

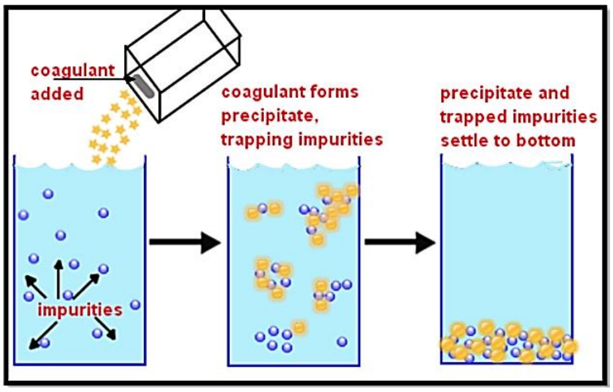

Figure 2.11: Coagulation-flocculation process combined with sedimentation (Redah, 2016).

2.3.4 Ion Exchange

Ion exchange method is basically to remove ionic species with the aid of an anionic, a cationic exchange resin or a combination of both. This method, also known as demineralization, is mostly employed to remove heavy metal ions from wastewater. Based on Figure 2.12, wastewater passes through a cation exchanger. Cations present in wastewater will be exchanged with hydrogen ions of resin and retained on exchanger. After stripping of carbon dioxide, the acidic wastewater passes through the anionic exchanger where negatively charged species will be stripped off by replacing themselves with hydroxide ions on resin.

On the other hand, pre-treatment of wastewater is necessary as the resin is sensitive to organic compounds. These compounds and waste produced may lead to fouling of exchangers irrespective to the resin types. Besides, high cost for resin maintenance and replacement as exchanger resin will be exhausted after long-period application (WasteWater System, 2011).

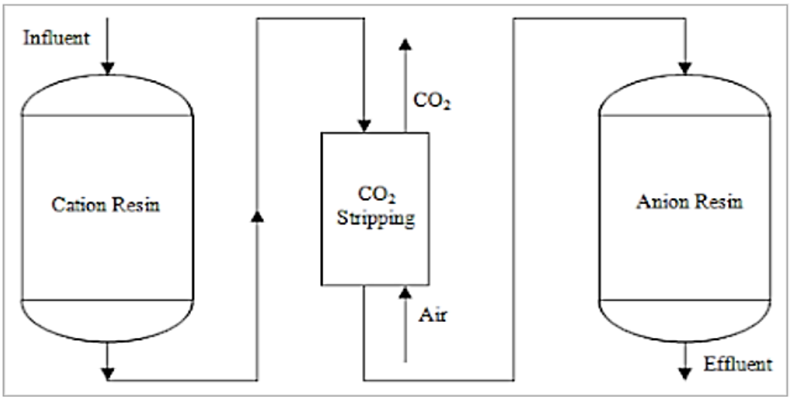

Figure 2.12: Schematic diagram of a typical demineralizer(WasteWater System, 2011).

2.3.5 Membrane Filtration

Membrane filtration is a physical method in separating species with particular size from solution or gaseous mixture with the aid of semi-permeable membrane. Nanofiltration is mostly used in dye removal due to highly effective, filter with appropriate pore size and simple operation. Pre-treatment upon membrane filter can be made in order to improve permeability, chemical resistance and microbial removal. Membrane bioreactor is incorporated in nanofiltration to remove organic compounds by degradation and easy sludge separation. Firstly, effluent undergoes pre-screening to remove larger sized particulates. The effluent is then passed to aeration tank for biological degradation of organic species including dye, flavonoids and polysaccharides. Next, the effluent will pass to membrane tank accompanied with a membrane bioreactor. As results, sludge is removed from membrane tank and aqueous effluent is disinfected (Ionics Freshwater Ltd., 2020).

Apart from that, one of the disadvantages of membrane filtration is a large amount of sludge will be produced. Fouling of membrane and high energy requirement are also problematic issues found in this method. Besides, maintenance and replacement cost become the consideration factors in wastewater treatment.

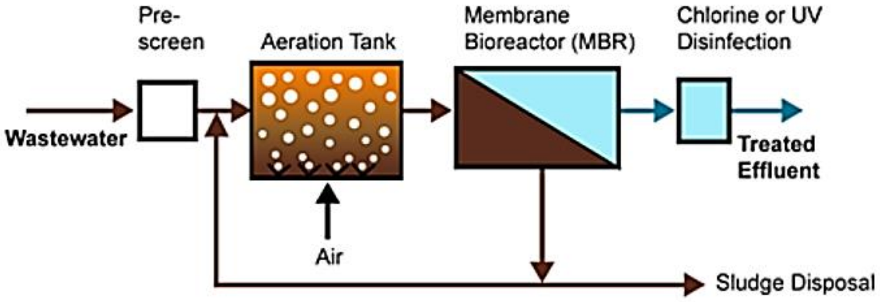

Figure 2.13: Membrane filtration with incorporation of membrane bioreactor (Ionics Freshwater Ltd., 2020).

2.4 Modelling of Kinetic and Adsorption Isotherm

In adsorption studies, pseudo-first and pseudo-second kinetic order models are mostly used in determining kinetic mechanisms based on the value of coefficient of determination, R^2. On the other hand, sorption isotherms define the binding patterns of dye molecules onto adsorbent surface.

2.4.1 Pseudo-First Order Kinetics

Pseudo-first order kinetic law was proposed by Lagergren in 19th century (1898). An adsorption process is said to obey the law when either one reagent present in excess in the system, while amount of the other remains constant. In other words, a bimolecular adsorption system performs as first-order reaction. Physisorption is expected to take place when the calculated R^2 value approaching to unity (Kajjumba, 2019). Physisorption is a reversible process which results from continuous formation and cleavage of weak bonds, such as hydrogen bonds and Van der Waals forces, between adsorbent and adsorbates.

2.4.2 Pseudo-Second Order Kinetics

In 18th century, pseudo-second order kinetic law was introduced and well known as it provided higher R^2 values for most results. In this case, both adsorbent and adsorbent active group will be participated in the slow step of an adsorption reaction. The reaction rate is strongly influenced by both reagents (Kajjumba, 2019). A good fit to the law indicating that chemisorption happens on adsorbent surface and strong chemical bonds such as ionic and covalent bonds are formed. As a result, it is an irreversible adsorption process.

2.4.3 Langmuir Isotherm

The applicability to Langmuir isotherm indicating that adsorbates are adhere onto adsorbent surface by aggregation into single layer. Each adsorption site can only occupy by one adsorbate in which further accommodation of another adsorbent is not possible. Based on Langmuir isotherm theory, adsorption and desorption rates are related to one another and depend on fraction of adsorbent surface. Besides, dimensionless separation factor, R_L describes the feasibility of an adsorption process (Ayawei, 2017).

2.4.4 Freundlich Isotherm

Freundlich isotherm is commonly used to describe the adsorption behavior involving heterogeneous surface. Apart from surface heterogeneity, it takes into accounts the adsorption site distribution and energy requirement. Similar to Langmuir isotherm, n value in Freundlich isotherm determines the favorability of the process. A good fit of it represents that multilayer of adsorbates aggregating on heterogeneous surface (Ayawei, 2017). Apart from interaction between adsorbates and adsorbent surface groups, bond formation or electrons transfer between adsorbates themselves is possible to occur.

CHAPTER 3

MATERIALS AND METHODOLOGY

3.1 Biosorbent Preparation

Cavendish bananas (*Musa acuminate*) were purchased from Tesco Kampar. The banana peels were cut into smaller pieces and washed thoroughly with distilled water to remove dust and impurities. The peels were dried in an oven at 70 °C for 5 hours. Then, the dried peels were grinded, sieved and kept in a desiccator for further use.

3.2 Adsorbate Preparation

Standard stock solution of Crystal Violet (CV) dye was prepared with concentration of 50 mg/L. The solution was kept in dark to prevent degradation of dye under light exposure.

3.3 Spectroscopy Analysis

Perkin Elmer FT-IR Spectrum RX1 was used to determine the presence of specific functional groups on banana peel surface before and after CV dye removal. The analyses were carried out using wavenumber range of 400 to 4000 cm^{-1}. Besides, topographies and morphologies of banana peel biosorbent surface, before and after dye adsorption, were analyzed via JEOL JSM 6701F FESEM and Park Systems EX-7 AFM respectively.

3.4 Batch Study

The following conditions were applied for batch adsorption experiment; 0.02 to 0.10 g of biosorbent dosage, 5 to 35 mg/L of initial dye concentration, 0 to 240 minutes of contact time and 2 to 10 of pH values. For each experiment, 0.1 g of banana peel powder (BPP) with 25 mL of CV dye solution (20 mg/L, pH = 6) in a 50 mL of centrifuge tube and an identical duplicate sample were agitated at 120 rpm for 180 minutes. The mixture was then centrifuged at 6000 rom for 5 minutes. Double beam UV/Visible spectrophotometer was used to determine both the initial and equilibrium concentration of dye solution at λ_{max} of 583 nm. The percent dye removal was calculated using the equation shown below:

$$\text{Percent removal (\%)} = \frac{C_0 - C_e}{C_0} \times 100\ \%$$

where C_0 and C_e are respective initial and equilibrium concentration of dye solution (mg/g).

3.4.1 Effect of Biosorbent Dosage

Amount of BPP was manipulated using 0.02, 0.04, 0.06, 0.08 and 0.10 g with 25 mL of CV dye solution (20 mg/L) in a 50 mL of centrifuge tube. Every mixture was agitated for 180 minutes at 120 rpm.

3.4.2 Effect of Initial pH

The pH of CV dye solution was adjusted to 2, 4, 6, 8 and 10 using hydrochloric acid (0.1 M and 1.0 M) and sodium hydroxide (0.1 M and 1.0 M). 0.10 g of BPP was added into 25 mL of pH-adjusted dye solution (20 mg/L) in a 50 mL of centrifuge tube. All mixtures were shaken for 180 minutes at 120 rpm.

3.4.2.1 Point of Zero Charge

Salt addition method (Inigo Babu *et al.*, 2016) was employed by first adjusting pH of 0.1 M of sodium nitrate solution with 0.1 M of sodium hydroxide and 0.1 M of nitric acid. 0.10 g of BPP was introduced into a 50 mL of centrifuge tube containing 25 mL of pH-adjusted salt solution. The agitation duration and speed were 24 hours and 120 rpm. The equation to calculate pH difference was expressed as following:

$$\Delta pH = pH_f - pH_i$$

where pH_f and pH_i represent final and initial pH of salt solution respectively.

3.4.3 Effect of Initial Concentration with Contact Time

50 mg/L of CV stock solution was diluted into 5, 20 and 35 mg/L. Similar to the procedure described in other adsorption parameters, 0.10 g of BPP was added into each centrifuge tube containing 25 mL of dye solution with respective dye concentration. The mixtures were agitated with speed of 120 rpm for 2, 4, 6, 8, 10, 15, 30, 45, 60, 120, 180 and 240 minutes.

3.4.4 Sorption Kinetics

Study of sorption kinetics was investigated by using initial CV dye concentrations of 5, 20 and 35 mg/L. Every dye solution was added 0.10 g of BPP and shaken for 180 minutes at 120 rpm. Pseudo-first and pseudo-second order kinetic models were used to evaluate the experimental data.

The equation of pseudo-first order kinetic model was shown as below:

$$\log(q_e - q_t) = \log q_e - \frac{k_1 t}{2.303}$$

where q_t and q_e are respective concentration of dye adsorbed at time t and at equilibrium (mg/g) and k_1 is the rate constant of pseudo-first order kinetic (min^{-1}).

The pseudo-second order equation was expressed as following:

$$\frac{t}{q_t} = \frac{1}{k_2 q_e^2} + \frac{t}{q_e}$$

where k_2 is the rate constant of pseudo-second order kinetic (min^{-1}) and $k_2 q_e^2$ is termed as initial sorption rate (mg/g min)

3.4.5 Sorption Isotherm

Sorption isotherm was studied by using adding 0.10 g of BPP into 25 mL of CV dye solution with concentration of 10, 15, 20, 25 and 35 mg/L. Each mixture was shaken for 180 minutes at 120 rpm. Both Langmuir and Freundlich isotherms were applied to predict the adsorption behavior.

The Langmuir isotherm equation was shown as following:

$$\frac{C_e}{q_e} = \frac{1}{q_m K_L} + \frac{C_e}{q_m}$$

where C_e is equilibrium dye concentration (mg/L), q_e is equilibrium concentration of dye adsorbed (mg/g), q_m is defined as maximum monolayer adsorption capacity (mg/g) and K_L is Langmuir sorption constant (L/mg).

In Langmuir isotherm, separation factor was an important variable to determine the favorability of an adsorption process. It was calculated by using equation shown below:

$$R_L = \frac{1}{1 + K_L C_0}$$

where C_0 represents the initial dye concentration (mg/L). The adsorption is favorable when $0 < R_L < 1$, unfavourable when $R_L > 1$, irreversible when $R_L = 0$ and linear when $R_L = 1$.

The Freundlich isotherm equation was expressed as below:

$$\log \mathrm{q_e} = \frac{1}{n} \log \mathrm{C_e} + \log \mathrm{K_F}$$

where K_F is Freundlich sorption constant (mg/g)(L/mg)$^{1/n}$ and *n* is extent of favorability of sorption in which the adsorption is favorable when *n* value is within 1 to 10.

CHAPTER 4

RESULTS AND DISCUSSION

4.1 Fourier-Transform Infrared (FT-IR) Analysis

FT-IR spectrum of raw banana peel powder (BPP) was depicted in Figure 4.1 (a). The broad and intense vibration band at 3422 cm^{-1} represented the O-H stretching of hydroxyl groups of polymeric components, including cellulose, hemicellulose, lignin and pectin. The respective bands appearing at 2926 cm^{-1} and 1635 cm $^{-1}$ reflected the C-H stretching of alkane and C=C stretching of aromatic rings (Mondal and Kar, 2018). Besides, C-H bending of lignin aromatic rings and C-N stretching for aliphatic amines showed the peaks at 1381 cm^{-1} (Alaa El-Din *et al*., 2017) and 1105 cm^{-1} (Deshmukh *et al*., 2017) respectively in the spectrum. Moreover, vibration band at 1034 cm^{-1} indicated the presence of C-O stretching of carboxylic acid, ester and alcohol as well (Memon *et al*., 2008). Lastly, the relatively low intensity peak at 617 cm^{-1} reflected the N-H deformation of amine groups (Dahiru *et al*., 2018).

By comparing both spectra, the vibration bands remain unshifted. The intensities of O-H, C-H, C=C, C-N, C-O stretching and N-H deformation were lower after Crystal Violet (CV) dye adsorption. It indicated that the functional groups mentioned previously involved in the adsorption process (Deshmukh *et al.*, 2017).

(a)

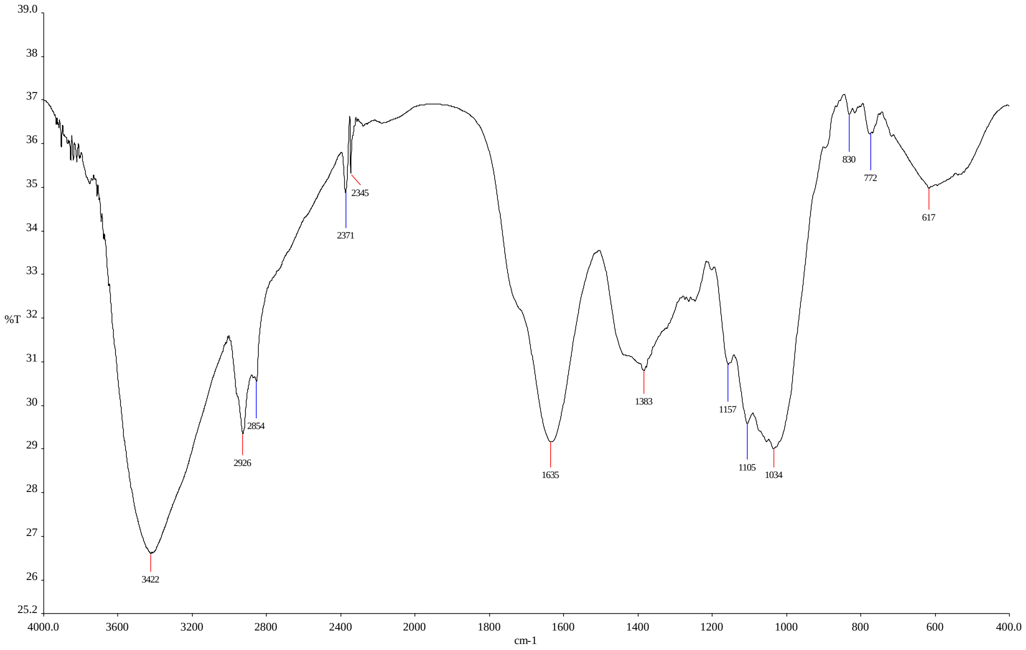

(b)

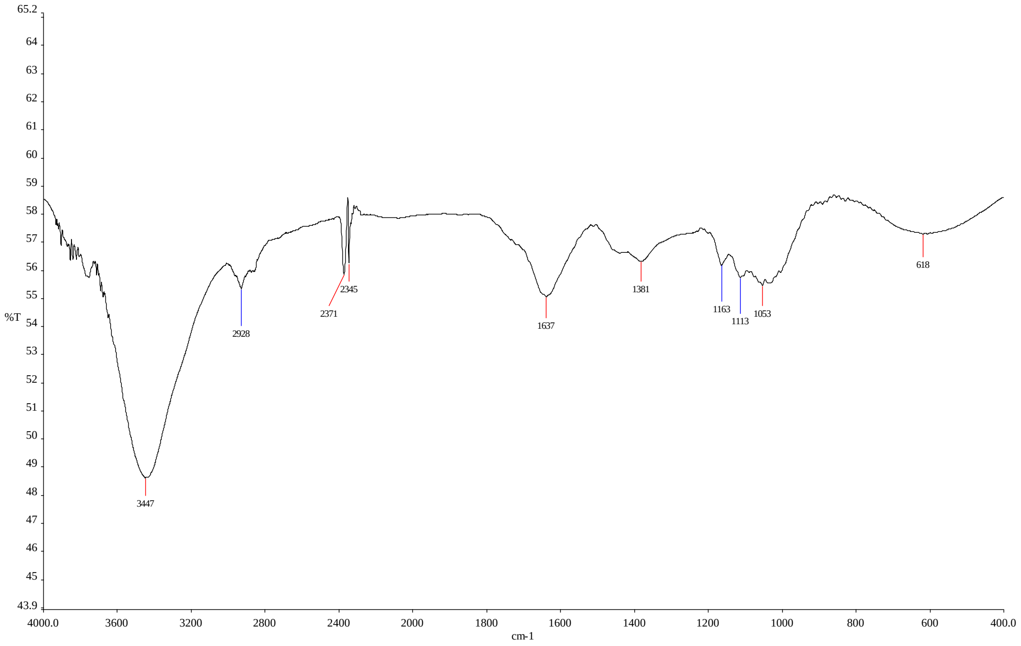

(c)

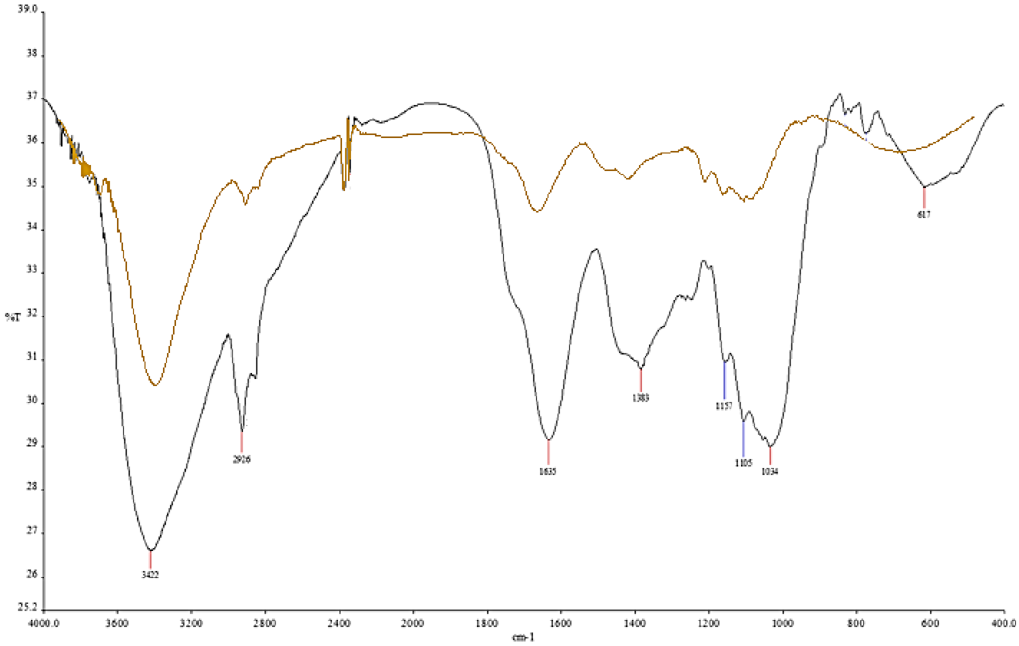

Figure 4.1: FT-IR spectra of BPP (a) before CV adsorption, (b) after CV adsorption and (c) by comparison (black and brown lines represent respective spectra before and after dye adsorption).

4.2 Scanning Electron Microscope (SEM) Analysis

Figures 4.2 (a) and (b) presented that the surface of raw BPP was rough and heterogeneous whereas it became smoother after CV dye uptake, as revealed in Figures 4.2 (c) and (d). The porous surface enhanced the adsorption of CV dye molecules (Hossain *et al.*, 2012). Other researchers, including Abdul Karim *et al.* (2016), Dahiru *et al.* (2018), Mondal and Kar (2018), Yusuff (2019), had reported the similar observation using different types of adsorbents and dyes.

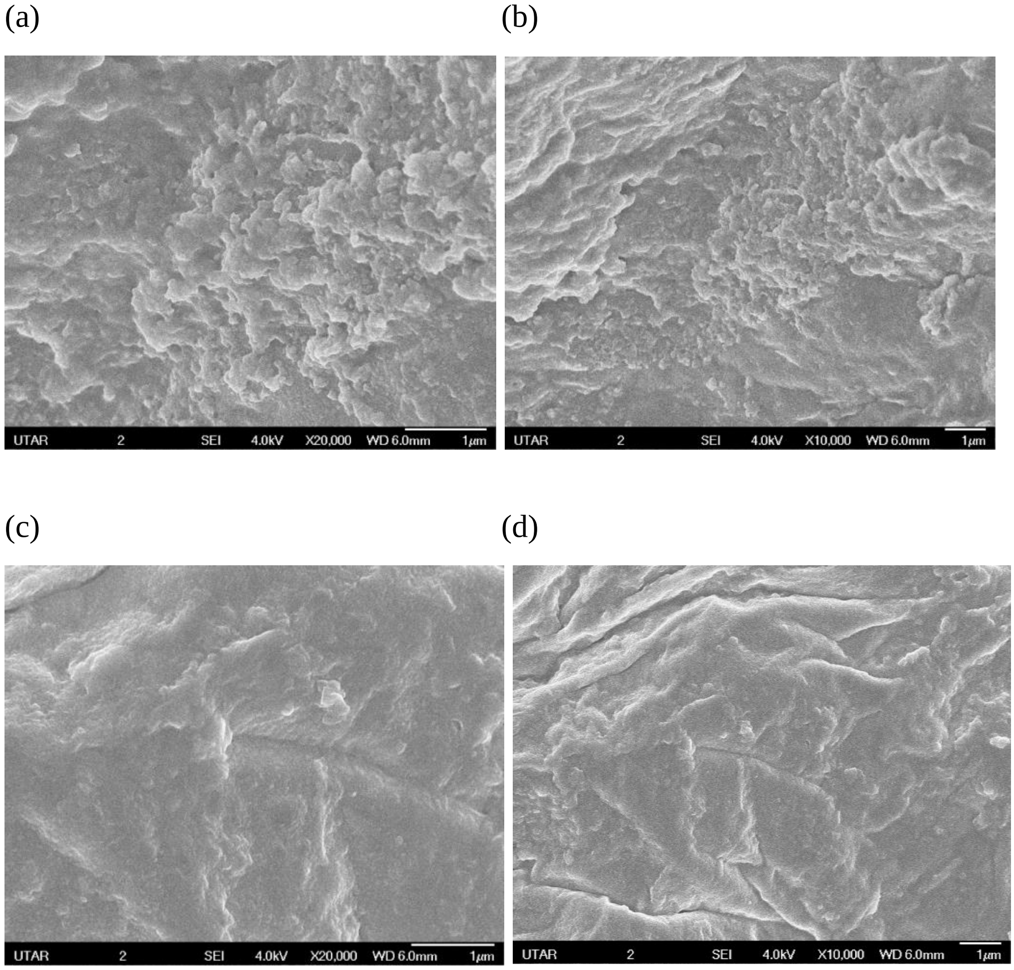

Figure 4.2: SEM images of raw BPP under magnification of (a) ×20000, (b) ×10000 and dye-adsorbed BPP under magnification of (c) ×20000, (d) ×10000.

4.3 Atomic Force Microscope (AFM) Analysis

From Figure 4.3 (a), it depicted that a regular grain-like structure was observed before CV dye uptake. The heterogeneous and porous surface facilitated the adhesion of CV dye molecules onto BPP (Hussein and Jasim, 2019). Furthermore, the structure of biosorbent after dye adsorption, as shown in Figure 4.3 (b), became rough and uneven. A darker coloured AFM topography was obtained after dye adsorption which indicated that the surface of BPP was saturated with CV dye molecules (Tay and Ong, 2019).

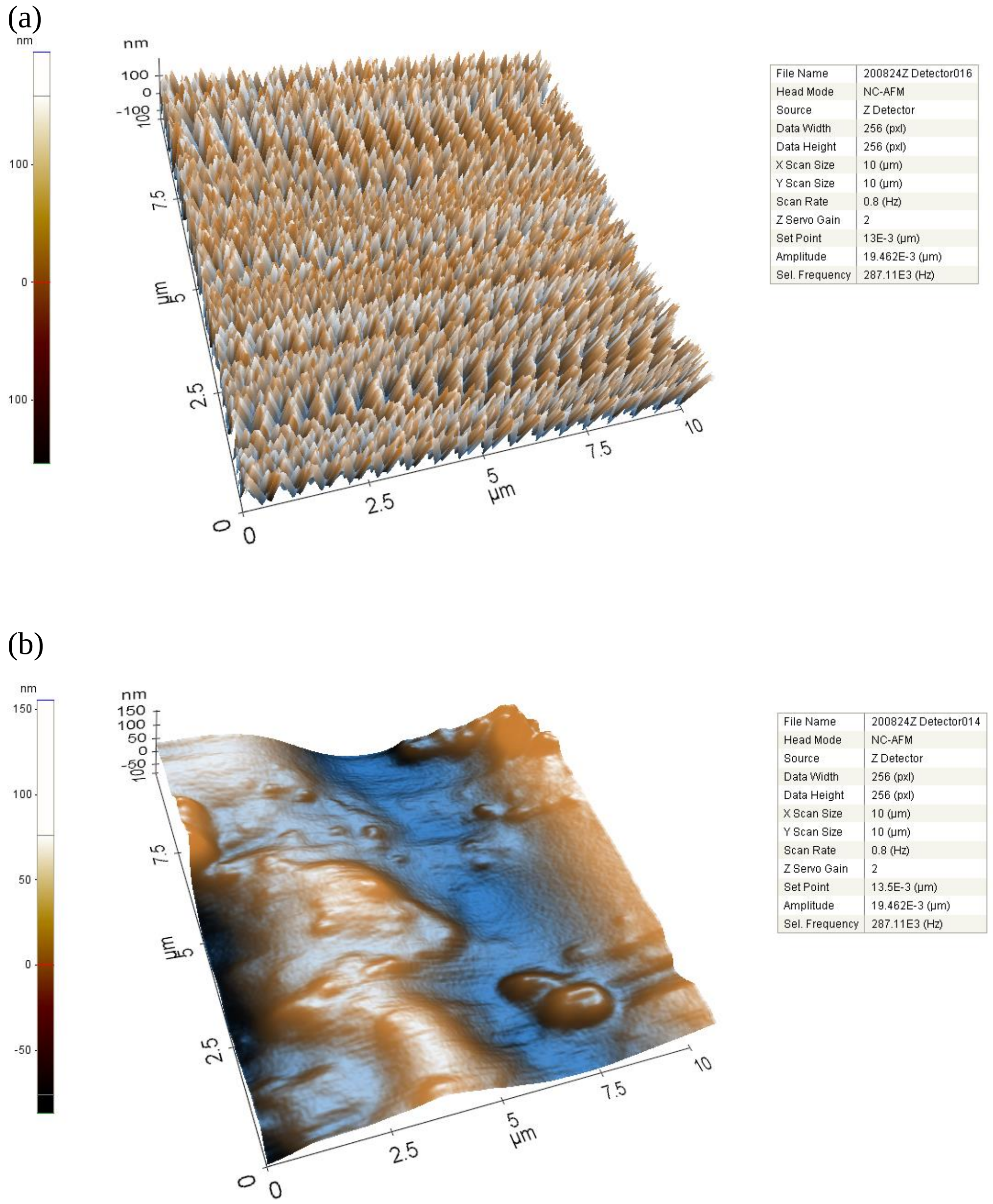

File Name	200824Z Detector016
Head Mode	NC-AFM
Source	Z Detector
Data Width	256 (pxl)
Data Height	256 (pxl)
X Scan Size	10 (µm)
Y Scan Size	10 (µm)
Scan Rate	0.8 (Hz)
Z Servo Gain	2
Set Point	13E-3 (µm)
Amplitude	19.462E-3 (µm)
Sel. Frequency	287.11E3 (Hz)

File Name	200824Z Detector014
Head Mode	NC-AFM
Source	Z Detector
Data Width	256 (pxl)
Data Height	256 (pxl)
X Scan Size	10 (µm)
Y Scan Size	10 (µm)
Scan Rate	0.8 (Hz)
Z Servo Gain	2
Set Point	13.5E-3 (µm)
Amplitude	19.462E-3 (µm)
Sel. Frequency	287.11E3 (Hz)

Figure 4.3: AFM images of BPP (10 µm × 10 µm) of BPP (a) before and (b) after CV dye adsorption.

4.4 Batch Study

4.4.1 Biosorbent Dosage

Based on Figure 4.4, it shown that the percentage of CV dye removal increased (more than 90 %) with biosorbent dosage up to 0.04 g. It indicated that maximum adsorption effect was achieved by using 0.02 to 0.04 g of adsorbent. The increase in percentage of dye removal resulted from an increase in number of vacant adsorption sites on biosorbent surface. Hence, more CV dye molecules could be adsorbed onto the surface (Dahiru *et al*., 2018). Further increase the dosage did not increase the percent dye removal. Conversely, the dye adsorption decreased using more biosorbent (1.0 g). It was probably because BPP tended to aggregate when there were relatively large amount of biosorbent present in the dye solution. The availability of adsorption sites decreased with a decrease in surface area of biosorbent (Garg *et al*., 2004; Pishgar *et al*., 2013).

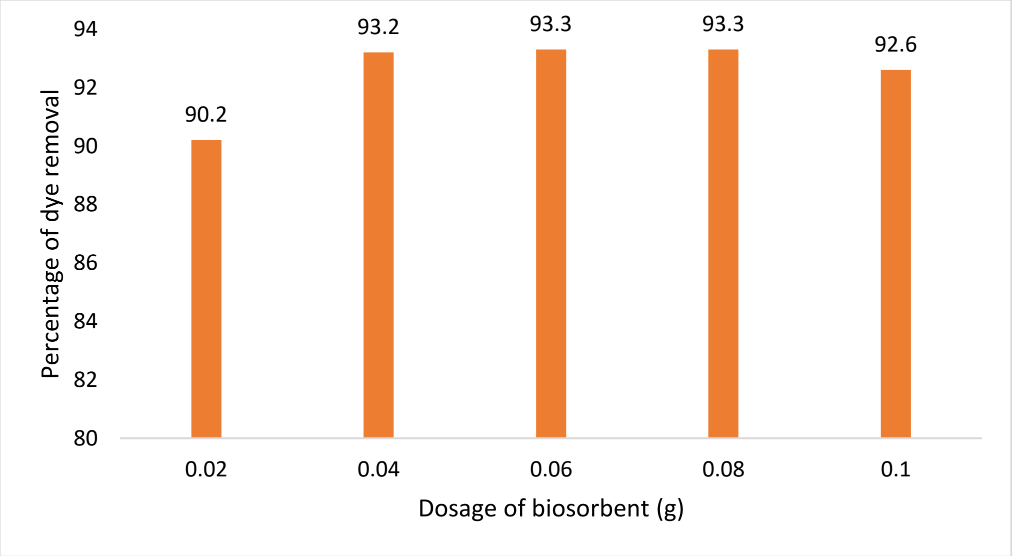

Figure 4.4: Effect of biosorbent dosage on CV dye removal.

4.4.2 Effect of Initial pH

The percentage of CV dye uptake was lower at pH 2.09 (87.8 %), as shown in Figure 4.5. At pH 4.30, the amount of dye uptake by BPP was the highest (92.4 %), followed by decreasing in percent dye removal until reaching the minimum adsorption amount at pH 10.70 (83.5 %).

Under extreme acidic condition, there were excess protons competing with CV dye molecules for the BPP surface. It led to lower interaction between dye molecules and the functional groups present on biosorbent surface. Within pH 4.30 to 9.20, the dye removal percent was higher (exceeded 90 %) due to significant electrostatic interaction between the negatively charged functional groups (O^- and COO^-) of BPP and positively charged amine groups ($-N^+(CH_3)_2$) of CV dye (Tay and Ong, 2019).

Conversely, the negative charge density of BPP reduced with increasing pH. There were repulsion forces exerted between positively charged biosorbent surface with the same charged of CV dye (Alshabanat *et al.*, 2013). Besides, CV dye achieved stability by delocalization of electrons between amine groups and the center carbon atom, forming stable tertiary carbocation (Kennepohl *et al.*, 2017) as shown in Figure 4.6. At high pH, the hydroxide ions would react with CV dye molecules. It caused diminishing of delocalization effect and the dye molecules existed as neutral form in the solution (Potrich and Amaral, 2017). Hence, the tendency for neutral dye molecules to adhere onto biosorbent surface was lower.

Moreover, the decrease in CV dye removal with an increase in initial pH of dye solution could be interpreted with the aid of point of zero charge, pH_{pzc} of BPP. Based on Figure 4.7, the pH_{pzc} of biosorbent was 5.20. According to experimental results, maximum CV dye adsorption took place at pH 4.30 (lower than pH_{pzc}). Researcher Mondal (2017) suggested that the electrostatic attraction between adsorbent and dye drove the adsorption process, leading to maximum adsorption effect.

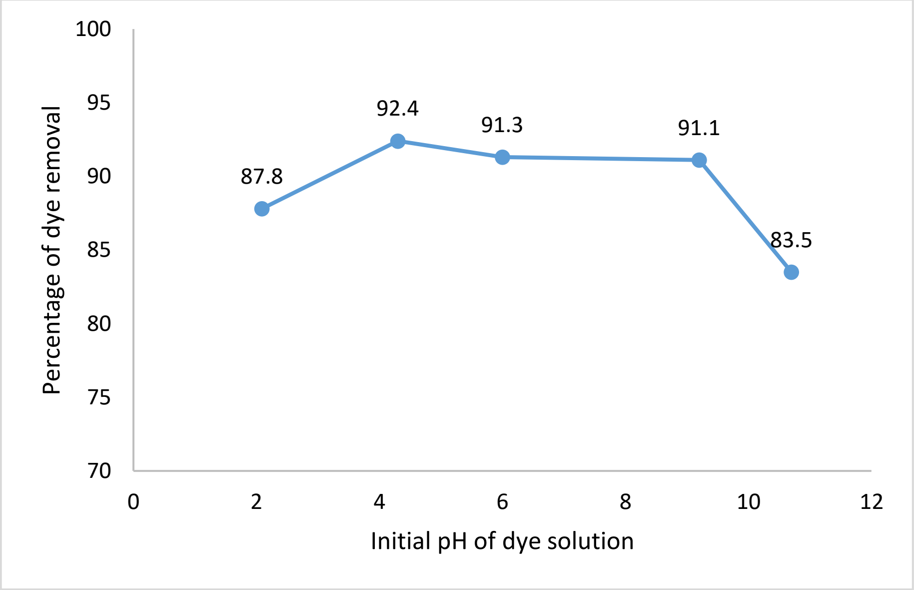

Figure 4.5: Effect of initial pH on CV dye uptake.

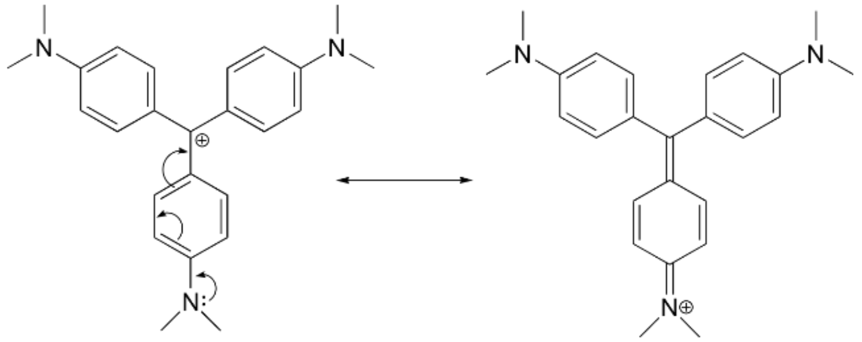

Figure 4.6: Resonance structures of CV dye.

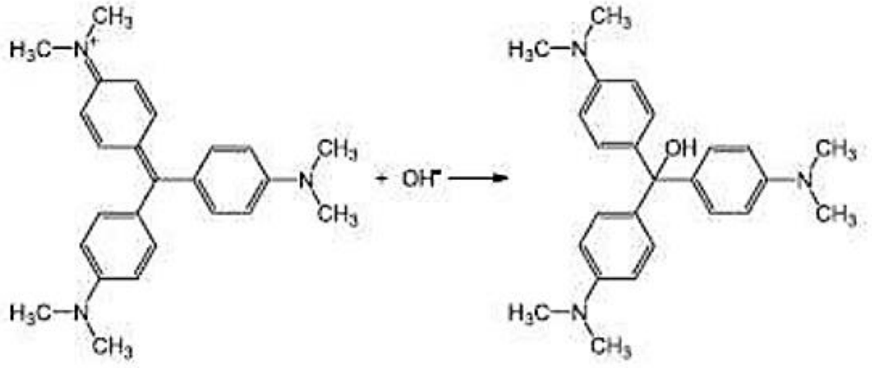

Figure 4.7: Schematic representation of reaction between CV dye and hydroxide ion.

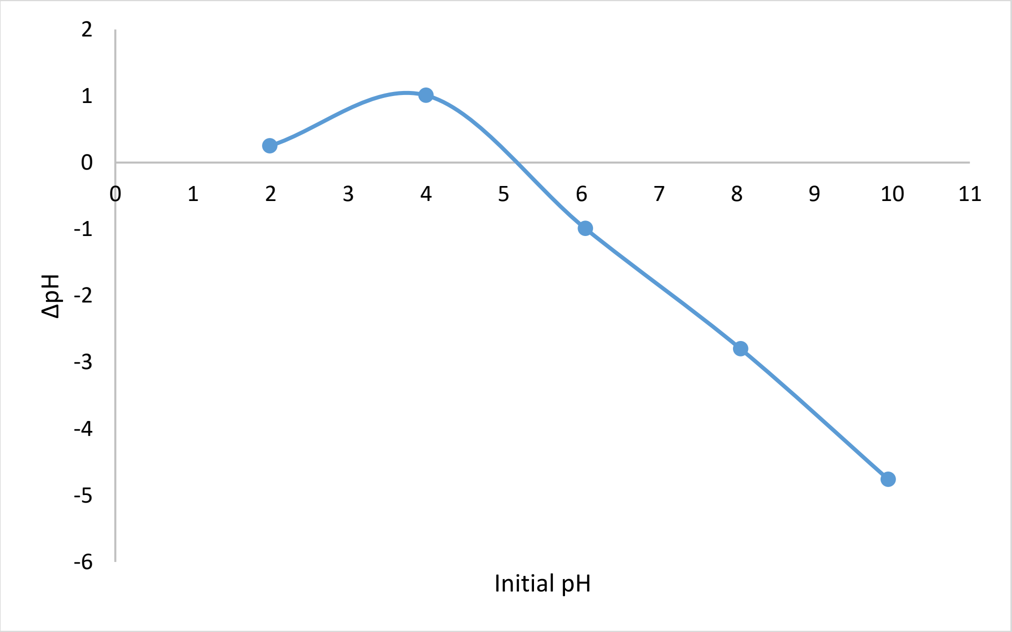

Figure 4.8: Point of zero charge of BPP.

4.4.3 Effect of Initial Concentration with Contact Time

According to Figure 4.9, the amount of CV dye removed was increased significantly at the early stage and eventually slowed down until saturation. Removal of dye increased sharply with increasing initial concentration of dye solution at initial stage was due to a large number of available adsorption sites on BPP (Das *et al*., 2014; Zadeh *et al*., 2018). At the same time, high concentration of CV dye solution acted as a driving force for the rapid adsorption. The adsorption slowed down gradually because the vacant adsorption sites reduced with time. Repulsive force between CV dye molecules was created as they were competing for the remaining adsorption sites on the surface of BPP (Wu *et al*., 2019).

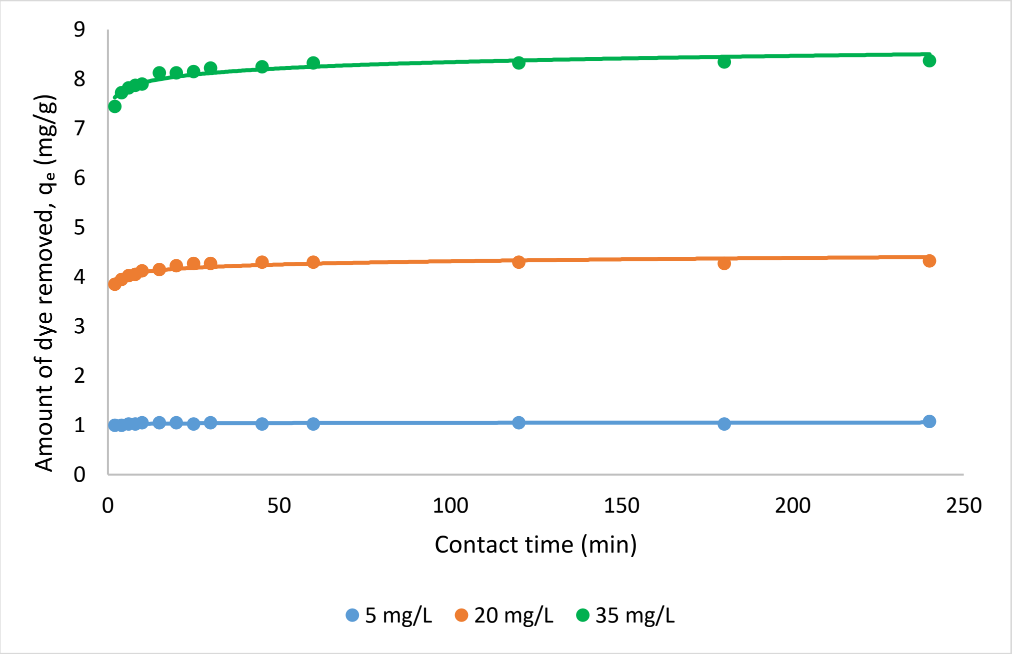

Figure 4.9: Effect of initial concentration on CV dye removal.

4.5 Sorption Kinetics

The parameters of pseudo-first (PFO) and pseudo-second order (PSO) kinetic models were determined from respective graphs of log ($q_e - q_t$) against t and $\frac{t}{q_t}$ against t, as depicted in Figures 4.10 and 4.11. The values were further tabulated in Table 4.1. For every initial CV dye concentration, coefficient of determination, R^2 value of PSO kinetic model was close to unity, whereas R^2 value for PFO kinetic model was much lower. Therefore, the adsorption behavior followed PSO kinetic model in which chemisorption took place in rate-determining step (Tay and Ong, 2019). Electrons were shared or exhanged between CV dye molecules and BPP surface active groups. In addition, Figure 4.12 showed that the difference between theoretical and experimental CV dye concentration at equilibrium was fairly small.

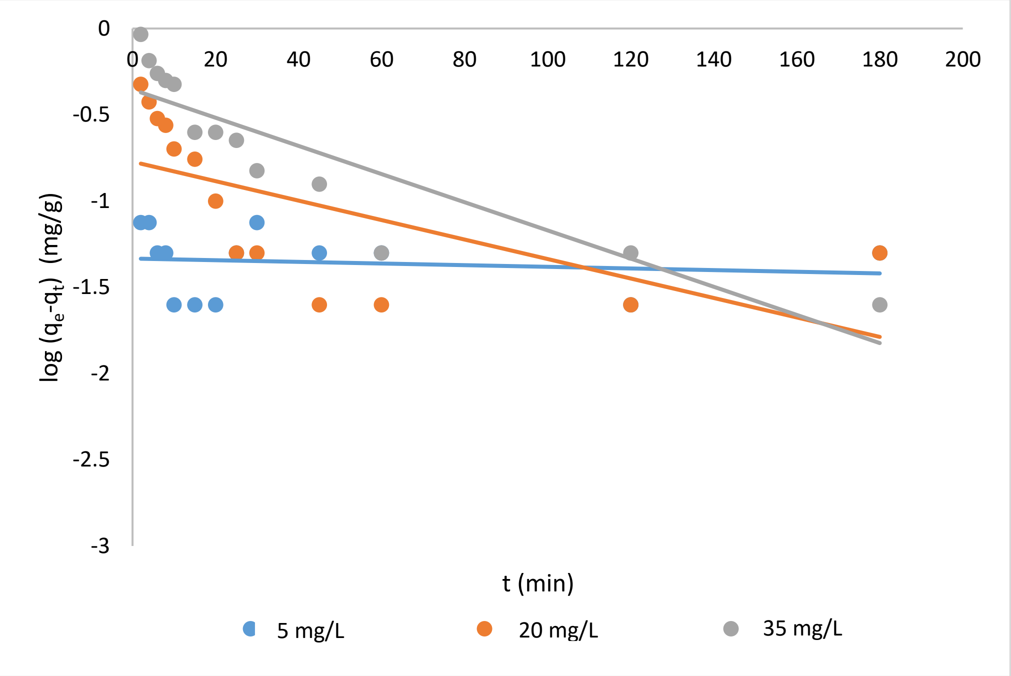

Figure 4.10: Pseudo-first order adsorption kinetic model.

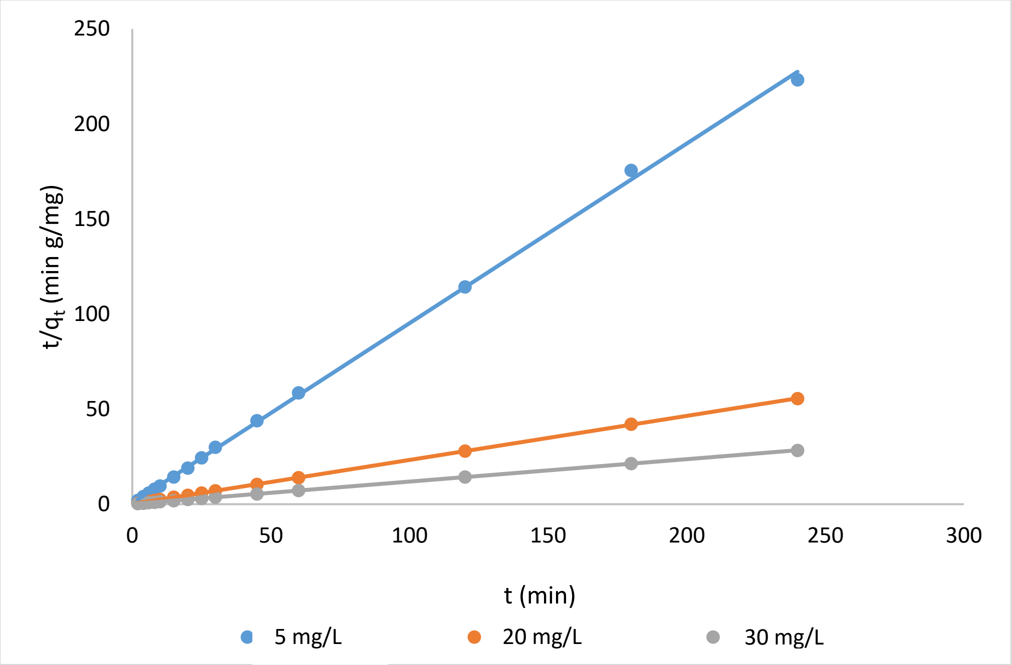

Figure 4.11: Pseudo-second order adsorption kinetic model.

Table 4.1: Parameters of pseudo-first and pseudo second order kinetic models for CV adsorption on BPP.

Parameters of kinetic models	Initial dye concentration, C_0 (mg/g)		
	5	20	35
Pseudo-first order:			
$q_{e\ exp}$ (mg/g)	1.075	4.325	8.375
$q_{e\ theo}$ (mg/g)	-1.3337	-0.7719	-0.3540
k_1 (min^{-1})	1.1515 x 10^{-3}	12.8968 x 10^{-3}	18.8846 x 10^{-3}
R^2	0.0182	0.3939	0.7960
Pseudo-second order:			
$q_{e\ exp}$ (mg/g)	1.075	4.325	8.375
$q_{e\ theo}$ (mg/g)	1.0586	4.3159	8.4816
k_2 (min^{-1})	1.2690	0.5754	0.1391
$k_2q_e^2$ (mg/g min)	1.4221	10.7180	10.0065
R^2	0.9993	1.0000	1.0000

*$q_{e\ exp}$ = experimental equilibrium concentration in unit of mg/g.
*$q_{e\ theo}$ = theoretical equilibrium concentration in unit of mg/g.

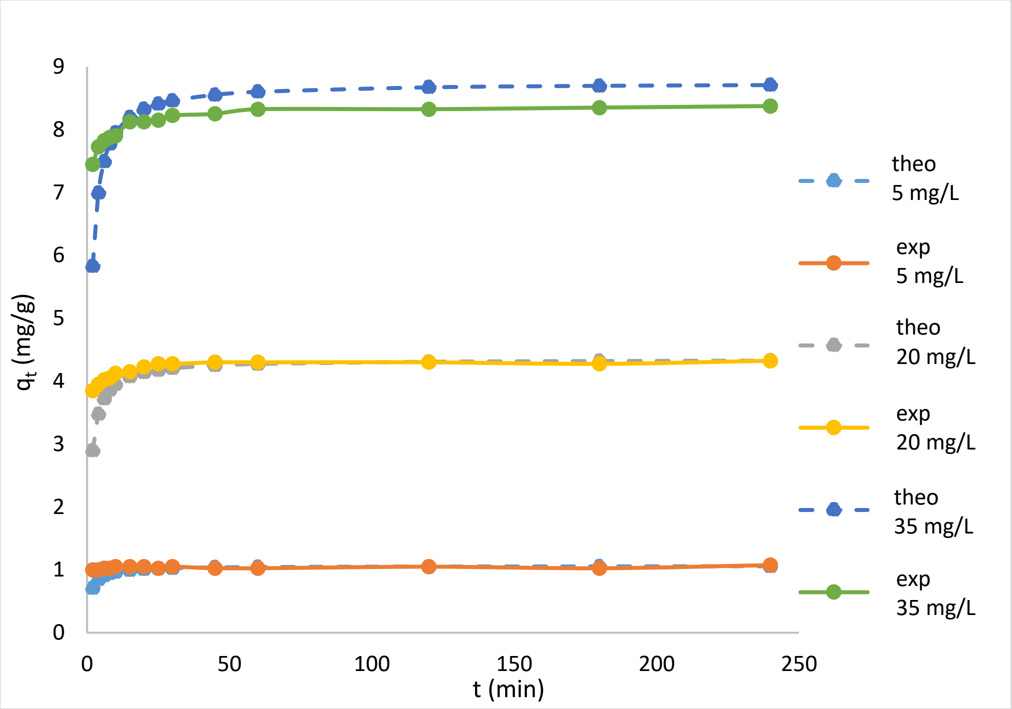

Figure 4.12: Comparison of experimental and theoretical equilibrium concentration with contact time.
*theo = theoretical, exp = experimental

4.6 Sorption Isotherm

R^2 value calculated using Freundlich isotherm equation (0.9569) was greater than that of Langmuir isotherm (0.7806). It was probably because the surface of BPP was heterogeneous, which could be confirmed from SEM analysis, and might have several types of binding sites for CV dye molecules (Wong, 2009). Besides, physisorption was leading (Kumar *et al*., 2011) at the initial stage of CV dye removal and supporting chemisorption to happen consequently on BPP surface (Richey *et al*., 2020). Meanwhile, the CV adsorption by BPP was favorable as the experimental *n* value lied within 1 to 10 (Hameed *et al*, 2008; Tay and Ong, 2019). Similar results reported by

Annadurai *et al*. (2002), Saechiam and Sripongpun (2019). The maximum adsorption capacity was 2.5763 mg/g.

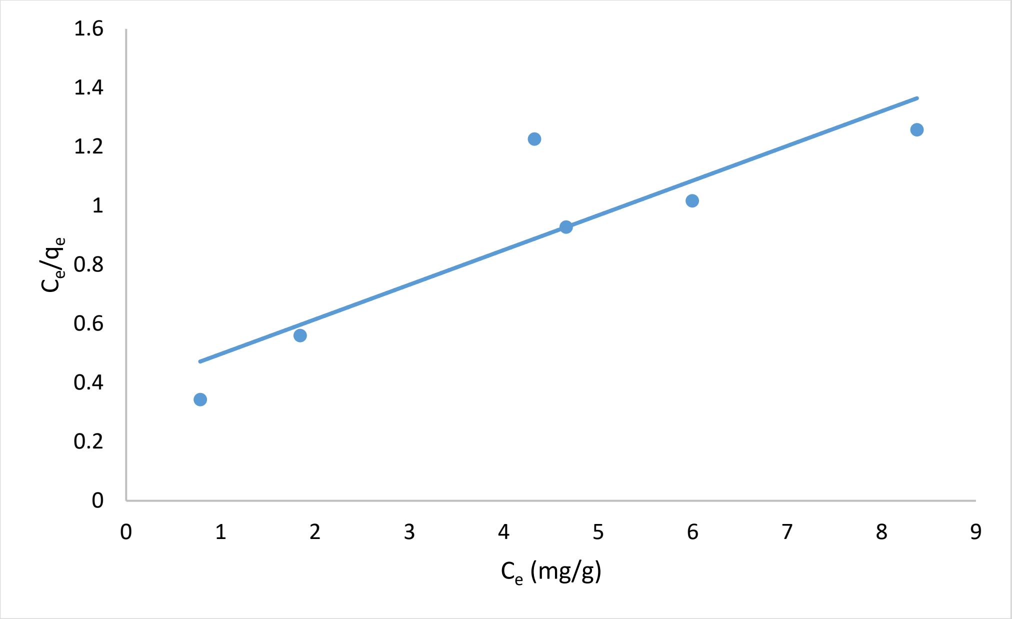

Figure 4.13: Langmuir isotherm of CV dye adsorption by BPP.

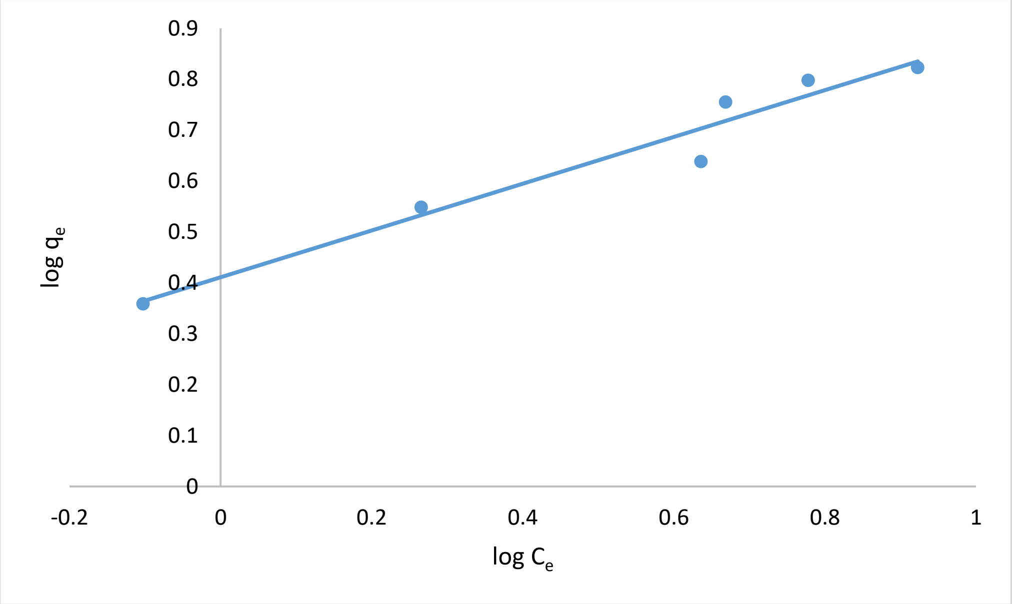

Figure 4.14: Freundlich isotherm of CV dye adsorption by BPP.

Table 4.2: Parameters and coefficient of determination of both isotherms in CV adsorption by BPP.

Langmuir isotherm			Freundlich isotherm		
K_L (mg^{-1})	q_m (mg/g)	R^2	K_F (mg/g)	*n*	R^2
0.9400	7.6046	0.7806	2.5763	2.1763	0.9569

CHAPTER 5

CONCLUSION

5.1 Conclusion

In conclusion, this study shows that BPP is a potential biosorbent in CV dye removal. FT-IR analysis revealed that the functional groups of BPP that involved in dye removal were O-H, C-H, C=C, C-N, C-O and N-H groups. Both SEM and AFM images depicted that the surface of raw BPP is heterogeneous with grain-like structure. The optimum biosorbent dosage and initial pH are 0.04 g and pH 4, respectively in order to achieve maximum CV adsorption onto BPP surface. The CV dye uptake increases sharply at the early stage of adsorption and decrease gradually until it approaches to equilibrium state. The experimental data fitted well in pseudo-second kinetic order mechanism with R^2 values of 0.9993, 1.000 and 1.000 for CV dye concentration of 5, 20 and 35 mg/g respectively. The isotherm data was well explained by Freundlich isotherm with 0.9569 and 2.1763 for R^2 and *n* values, respectively. The maximum adsorption capacity is 2.5763 mg/g.

5.2 Recommendation for Future Study

Recommendation are proposed to have better understanding on the adsorption behavior of BP in dye removal process as well as improve efficiency of BP as a biosorbent in wastewater treatment. Firstly, other adsorption kinetic modelling such as Elovich, intraparticle diffusion, Brunauer, Emmett and Telle (BET) isotherm can be performed to help in predict the binding modes of CV dye molecules onto BP surface. Besides, thermodynamic studies can be conducted to investigate the feasibility of CV dye removal by BP biosorbent. Moreover, modification of BP surface active groups can be made in order to enhance adsorption ability regards to different classes of dyes. In addition, mobilization of BP is important for easier separation of biosorbent from dye solution. Last but not least, desorption mechanism of BP should be studied to recover the adsorbed BP and re-use in the dye adsorption process.

REFERENCES

Abdul Karim, S.K. et al., 2016. Banana fibers as sorbent for removal of Acid Green dye from water', *Journal of Chemistry*.

Abrahart, E.N. and Stothers, J.B., 2017. *Dyes* [Online]. Available at: https://www.britannica.com/technology/dye [Accessed: 8 August 2020].

Ahmad, R., 2009. Studies on adsorption of Crystal Violet dye from aqueous solution onto *Coniferous Pinus* bark powder (CPBP). *Journal of Hazardous Materials*, 171, pp. 767 – 773.

Alaa El-Din, G., Amer, A.A., Malsh, G. and Hussein, M., 2017. Study on the use of banana peels for oil spill removal. *Alexandria Engineering Journal*, 57(3), pp. 2061 – 2068.

Alshabanat, M., Alsenani, G. and Almufarij, R., 2013. Removal of Crystal Violet dye from aqueous solutions onto date palm fiber by adsorption technique. *Journal of Chemistry*.

Amel, K., Hassena, M.A. and Kerroum, D., 2012). Isotherm and Kinetics Study of Biosorption of Cationic Dye onto Banana Peel. *Energy Procedia*, 19, pp. 286 – 295.

Annadurai, G., Juang, R.S. and Lee, D.J., 2002. Use of cellulose-based wastes for adsorption of dyes from aqueous solutions. *Journal of Hazardous Materials B92*, pp. 263 – 274.

Aspland, J.R., 1992. Vat dyes and their application. *Textile Chemist & Colorist*, 24(1), pp. 22 – 24.

Ayawei, N., Ebelegi, A.N. and Wankasi, D., 2017. Modelling and interpretation of adsorption isotherms. Journal of Chemistry.

Bhatia, D., Sharma, N.R., Singh, J. and Kanwar, R.S., 2017. Biological methods for textile dye removal from astewater: a review. *Critical Reviews in Environmental Science and Technology*, pp. 1 – 41.

Carreon-Valencia, T. et al., 2008. General introduction to the chemistry of dyes. In: *IARC working group on the evaluation of carcinogenic risks to humans: Some aromatic amines, organic dyes, and related exposures*. Lyon: International Agency for Research on Cancer, pp. 55 – 68.

Chakraborty, S., Chowdhury, S. and Saha, P.D., 2011. Adsorption of Crystal Violet from aqueous solution onto NaOH-modified rice husk. *Carbohydrate Polymers*, 86, pp. 1533 – 1541.

Chan, S.L., Tan, Y.P., Abdullah, A.H. and Ong, S.T., 2016. Equilibrium, kinetic and thermodynamic studies of a new potential biosorbent for the removal of Basic Blue 3 and Congo Red dyes: pineapple (*Ananas comosus*) plant stem. *Journal of the Taiwan Institute of Chemical Engineers*, 61, pp. 306 – 315.

Chequer, F.M.D. et al., 2013. Textile dyes: Dyeing process and environmental impact. In: Gunay, M. (ed.). *Eco-friendly textile dyeing and finishing*. Croatia: Intech, pp. 151 – 234.

Dahiru, M., Zango, Z.U. and Haruna, M.A., 2018. Cationic dyes removal using low-cost banana peel biosorbent. *American Journal of Materials Science*, 8(2), pp. 32 – 38.

Das, B., Mondal, N.K., Bhaumik, R. and Roy, P., 2014. Insight into adsorption equilibrium, kinetics and thermodynamics of lead onto alluvial soil. *International Journal of Environmental Science and Technolog*y, 11, pp. 1101 – 1114.

Deshmukh, P.D., Khadse, G.K., Shinde, V.M. and Labhasetwar, P., 2017. Cadmium removal from aqueous solutions using dried banana peels as an adsorbent: Kinetics and equilibrium modeling. *Journal of Bioremediation & Biodegradation*, 8(3).

Dutta, M., Mishra, S., Kaushik, M. and Basu, J.K., 2011. Application of Various Activated Carbons in the Adsorptive Removal of Methylene Blue from Aqueous Solution. *Research Journal of Environmental Sciences*, 5, pp. 741 – 751.

Garg, V.K., Kumar, R. and Gupta, R., 2004. Removal of Malachite Green dye from aqueous solution by adsorption using agro-industry waste: a case study of *Prosopis cineraria*. *Dyes and Pigments*, 62(1), pp. 1 – 10.

Hameed, B.H., Mahmoud, D.K. and Ahmad A.L, 2008. Equilibrium modeling and kinetic studies on the adsorption of basic dye by a low-cost adsorbent: Coconut (*Cocos nucifera*) bunch waste. *Journal of Hazardous Materials*, 158, pp. 65 – 72.

Hossain, M.A., Hao Ngo, H., Guo, W.S. and Nguyen, T.V., 2012. Removal of copper from water by adsorption onto banana peel as bioadsorbent. *International Journal of Geomate*, 2(2), pp. 227 – 234.

Hunger, K., 2003. *Industrial dyes: chemistry, properties, applications*. 3rd ed. Kelkheim: Wiley-VCH.

Hussein, T.K. and Jasim, N.A., 2019. Removal of Crystal Violet and Methylene Blue from synthetic industrial wastewater using fennel seed as an adsorbent. *Journal of Engineering Science and Technology*, pp. 2947 – 2963.

Hussin, Z.M., Talib, N., Hussin, N.M., Hanafiah, M.A.K.M and Khalir, W.K. A.W.M., 2015. Methylene Blue adsorption onto NaOH modified durian leaf powder: isotherm and kinetic studies. *American Journal of Environmental Engineering*, 5(3A): pp. 38 – 43.

Inigo Babu, I. et al., 2016. Removal of Crystal Violet dye from water using banana peel charcoal and AMPS-g-banana peel charcoal hydrogels: a comparative study. *South Asian Journal of Engineering and Technology*, 2(24), pp. 155 – 168.

Inoue, K. et al., 2017. Biosorbents for Removing Hazardous Metals and Metalloids. *Materials (Basel)*, 10(8).

Ionics Freshwater Ltd., 2020, *Wastewater treatment* [Online]. Available at: http://www.ionicsfreshwater.com/index.php/wastewater-treatment [Accessed: 21 August 2020].

Kajjumba, G.W. et al., 2019. Modelling of adsorption kinetic processes – errors, theory and application. In: Edebali, S. (ed.). Advanced sorption process application. London: IntechOpen.

Kamar, F.H. et al., 2018. Use of artificial neural network for modeling and prediction of Reactive Red dye removal from wastewater using banana peels bio-sorbent. *Revista de Chimie (Bucharest)*, 69(8), pp. 1919 – 1926.

Kennepohl, D., Farmer, S. and Soderberg, T, 2017, *Carbocation Structure and Stability* [Online]. Available at: https://courses.lumenlearning.com/suny-mcc organicchemistry/chapter/carbocation-structure-and-stability/ [Accessed: 25 August 2020].

Khaled, A., Nemr, A.E., Sikaily, A.S. and Abdelwahab, O., 2009. Removal of Direct N Blue-106 from artificial textile dye effluent using activated carbon from orange peel: Adsorption isotherm and kinetic studies. *Journal of Hazardous Materials*, 165(1 – 3), pp. 100 – 110.

Knoema., 2018, *Malaysia - bananas production quantity* [Online]. Available at: https://knoema.com/atlas/Malaysia/topics/Agriculture/Crops-Production-Quantity-tonnes/Bananas-production [Accessed: 25 August 2020].

Kooh, M.M.R., Dahri, M.K. and Lim, L.B.L., 2016. The removal of Rhodamine B dye from aqueous solution using *Casuarina equisetifolia* needles as adsorbent. *Cogent Environmental Science*, 2(1).

Krysztafkiewicz, A., Binkowski, S. and Jesionowski, T., 2002. Adsorption of dyes on a silica surface. *Applied Surface Science*, 199, pp. 31 – 39.

Kuehni, R.G., Plains, S. and Cox, T.C., Mobay Chemical Corporation, 1982. *Levelling agent and process of levelling for the disperse dyeing of hydrophobic materials*. U.S. Pat. 4,341,526.

Lagergren, S., 1898. Zur theorie der sogenannten adsorption geoster stoffe, Kungliga Svenska Vetenskapsakad. *Handlingar*, 24(4), pp. 1 – 39.

Loulidi, I. et al., 2020. Adsorption of Crystal Violet onto an agricultural waste residue: kinetics, isotherm, thermodynamics, and mechanism of adsorption. *The Scientific World Journal*.

Mahapatra, N.N., 2016. *Textile dyes*. New Delhi: Woodhead Publishing India Pvt. Ltd.

Matyjas, E. and Rybicki, E., 2003. Novel reactive red dyes. *Autex Research Journal*, 3(2), pp. 90 – 95.

Memon, J.R., Memon, S.Q., Bhanger, M.I. and Khuhawar, M.Y., 2008. Banana peel: a green and economical sorbent for Cr(III) removal. *Pakistan Journal of Analytical and Environmental Chemistry*, 9(1), pp. 20 – 25.

Mondal, N.K. and Kar, S., 2018. Potentiality of banana peel for removal of Congo Red dye from aqueous solution: isotherm, kinetics and thermodynamics studies. *Applied Water Science*, 157.

Mondal, N.K., 2017. Natural banana (*Musa acuminate*) peel: an unconventional adsorbent for removal of fluoride from aqueous solution through batch study. *Water Conservation Science and Engineering*, 1, pp. 223 – 232.

Munagapati, V.S., et al., 2019. Adsorptive removal of anionic dye (Reactive Black 5) from aqueous solution using chemically modified banana peel powder: kinetic, isotherm, thermodynamic, and reusability studies. *International Journal of Phytoremediation*.

Nadiah, R., 2018, *Today's trend, tomorrow's trash* [Online]. Available at: https://www.nst.com.my/amp/lifestyle/pulse/2018/05/370987/todays-trend-tomorrows-trash [Accessed: 23 August 2020].

Namasivayam, C. and Kavitha, D., 2002. Removal of Congo Red from water by adsorption onto activated carbon prepared from coir pith, an agricultural solid waste. *Dyes and Pigments*, 54, pp. 47 – 58.

Nathanson, J.A. and Ambulkar, A., 2010, *Wastewater treatment* [Online]. Available at: https://www.britannica.com/technology/wastewater-treatment [Accessed: 30 August 2020].

Ofomaja, A.E., 2007. Sorption dynamics and isotherm studies of Methylene Blue uptake on to palm kernel fibre. *Chemical Engineering Journal*, 126, pp. 35 – 43.

Ohba, N. et al., Nihon Surfactant Kogyo K.K., 1990. *Dyeing auxiliary composition: levelling agent for reactive dyes containing hydroxy sulfonic acid anionic surfactant and poly-basic polymer*. U.S. Pat. 4,976,743.

Papirio, S. et al., 2017. Heavy metal removal from wastewaters by Biosorption: mechanisms and modeling. In: Rene, E.R., Sahinkaya**,** E., Lewis, A., Lens, P. (eds.). *Sustainable Heavy Metal Remediation: Volume 1: Principles and Processes*. Cham: Springer International Publishing, pp. 25 – 63.

Pishgar, M., Yazdanshenas, M.E., Ghorbani, M.H. and Farizadeh, K., 2013. Removal of Basic Blue 159 from aqueous solution using banana peel as a low-cost adsorbent. *Journal of Applied Chemical Research*, 7(4), pp. 51 – 62.

Pollution Control Department, 2017. *Water quality standards* [Online]. Available at: http://www.pcd.go.th/ info_serv/en_reg_std_water04.html/ [Assessed: 12 August 2020].

Potrich, E. and Amaral, L.S., 2017. Determination of kinetic parameters of the Crystal Violet reaction with sodium hydroxide applying absorbance technique and the laws of Lambeert-Beer and Arrhenius. *Enciclopédia Biosfera*, 14(25), pp. 1852 – 1861.

Prabhu, K.H. and Bhute, A.S., 2012. Plant based natural dyes and mordants: A review. *Journal of Natural Product and Plant Resources*, 2(6), pp. 649 – 664.

Rajeshkannan, R., Rajasimman, M. and Rajamohan, N., (2011). Decolourization of Malachite Green using tamarind seed: optimization, isotherm and kinetic studies. *Chemical Industry & Chemical Engineering Quarterly*, 17(1), pp. 67 – 79.

Redah, M.A., 2016. *Wastewater treatment using successive electrochemical approaches*. PhD Thesis, University of Baghdad, Iraq.

Richards, P.R., 2012. Dye types and application methods. In: Best, J. (ed.). *Colour design: theories and applications*. Duxford: Woodhead Publishing, pp. 471 – 496.

Richey, N.E., Paula, C.D. and Bent, S.F., 2020. Understanding chemical and physical mechanisms in atomic layer deposition. *The Journal of Chemical Physics*, 152(4).

Saechiam, S. and Sripongun, G., 2019. Adsorption of Malachite Green from synthetic wastewater using banana peel adsorbents. *Songklanakarin Journal of Science and Technology*, 41(1), pp. 21 – 29.

Samer, M., 2015. Biological and chemical wastewater treatment processes. In: Samer, M. (ed.). *Wastewater treatment engineering*. Rijeka: InTech, pp. 1 – 50.

Scaccia, R.L., Coughlin, D. and Ball, D.W., 1998. A microscale synthesis of Mauve. *Journal of Chemical Education*, 75(6).

Sharifuddin, S.S. and Ang, S.Y., 2017, *Current situation and issues of industrial wastewater management in Malaysia* [Online]. Available at: http://wepa-db.net/3rd/en/meeting/20170926/pdf/26_3-06_Malaysia.pdf [Accessed: 23 August 2020].

Shukla, S.R., 2007. Pollution abatement and waste minimization in textile dyeing. In: Christie, R.M. (ed.). *Environmental aspects of textile dyeing*. Cambridge: Woodhead Publishing Limited, pp. 116 – 148.

Stavrinou, A., Aggelopoulos, C.A. and Tsakiroglou, C.D., 2018. Exploring the adsorption mechanisms of cationic and anionic dyes onto agricultural waste peels of banana, cucumber and potato: adsorption kinetics and equilibrium isotherms as a tool. *Journal of Environmental Chemical Engineering*, 6(6), pp. 6958 – 6970.

Sumalapao, D.E.P. et al., 2016. Biosorption kinetic models on the removal of Congo Red onto unripe Calamansi (*Citrus Microcarpa*) peels. *Oriental Journal of Chemistry*, 32(6).

Tafesse, T.B., Yetemegne, A.K. and Kumar, S., 2015. Analysis of copper, chromium & lead in Hawassa and Arba Minch textile effluents. *Journal of Chemistry and Chemical Sciences*, 5(4), pp. 153 – 168.

Tahir, H., Hammed, U., Sultan, M. and Jahanzeb, Q., 2010. Batch adsorption technique for the removal of Malachite Green and Fast Green dyes by using montmorillonite clay as adsorbent. *African Journal of Biotechnology*, 9(48), pp. 8206 – 8214.

Tahir, H., Sultan, M. and Jahanzeb, Q., 2008. Removal of basic dye Methylene Blue by using bioabsorbents *Ulva lactuca* and *Sargassum*. *African Journal of Biotechnology*, 7(15), pp. 2649 – 2655.

Tanzim, K. and Abedin, M.Z., 2015. Adsorption of Methylene Blue from aqueous solution by pomelo (*Citrus maxima*) peel. *International Journal of Scientific & Technology Research*, 4(12), pp. 230 – 232.

Tay, C.I. and Ong, S.T., 2019. Guava leaves as adsorbent for the removal of emerging pollutant: ciprofloxacin from aqueous solution. *Journal of Physical Science*, 30(2), pp. 137 – 156.

Thomas, G. and Udo, M., 2000. Triarylmethane and diarylmethane dyes. In: *Ullmann's Encyclopedia of Industrial Chemistry*. New Yok: Wiley-VCH..

Vital, R.K., Saibaba, K. V. N., Shaik, K. B. and Gopinath, R., 2016. Dye removal by adsorption: A review. *Journal of Bioremediation and Biodegradation*, 7(371).

Wang, J.L. and Chen, C., 2009. Biosorbents for heavy metals removal and their future. *Biotechnology Advances*, 27, pp. 195 – 226.

WasteWater System, 2011. *Ion exchange application in wastewater treatment* [Online]. Available at: http://www.wastewatersystem.net/2011/08/ion-exchange-application-in-wastewater.html [Assessed: 03 September 2020].

Weckler, G., Hauss, H.J., Hintermeier, K. and Engelhardt, F., Cassella Aktiengesellschaft, 1981. *Levelling agent and process for the even dyieng of materials made of synthetic fibers*. U.S. Pat. 4,250,296.

Wong, S.Y., Tan, Y.P., Abdullah, A.H. and Ong, S.T., 2009. Removal of Basic Blue 3 and Reactive Orange 16 by adsorption onto quartenized sugar cane bagasse. *The Malaysian Journal of Analytical Sciences*, 13(2), pp. 185 – 193.

Wu, H.F. et al., 2019. Synthesis of activated carbon from peanut shell as dye adsorbents for wastewater treatment. *Adsorption Science & Technology*, 37(1-2), pp. 34 – 48.

Yaacob, M.R. et al., 2015. Environmental awareness of batik entrepreneurs in Kelantan, Malaysia – An early insight. *International Journal of Academic Research in Business and Social Sciences*, 5(4), pp. 338 – 347.

Yang, Y.Y. et al., 2011. Competitive biosorption of Acid Blue 25 and Acid Red 337 onto unmodified and CDAB-modified biomass of *Aspergillus oryzae*. *Bioresource Technology*, 102, pp. 7429 – 7436.

Yusuff, A.S., 2019. Adsorption of cationic dye from aqueous solution using composite chicken eggshell - anthill clay: optimization of adsorbent preparation conditions. *Acta Polytechnica*, 59(2), pp. 192 – 202.

Zadeh, B.S., Esmaeili, H. and Foroutan, R., 2018. Cadmium (II) removal from aqueous solution using microporous eggshell: kinetic and equilibrium studies. *Indonesian Journal of Chemistry*, 18(2).

Zhou, Y.Z., Ge, L.Q. and Fan, N., 2018. Adsorption of Congo Red from aqueous solution onto shrimp shell powder. *Adsorption Science & Technology*, 36(5-6), pp. 1310 – 1330.

APPENDICES

APPENDIX A

Calibration Curve of CV Standard Solution

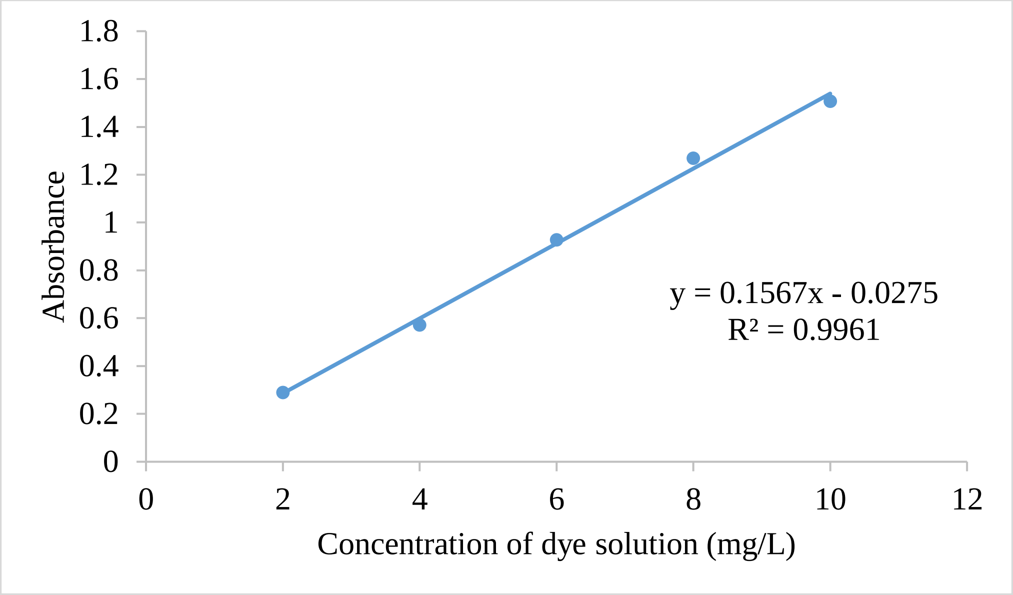

APPENDIX B

Effect of BPP Biosorbent Dosage on Percentage of CV Removal

Dosage of biosorbent (g)	Absorbance (A)	Initial concentration (mg/L)	Equilibrium concentration (mg/L)	Percentage of dye removal (%)
0.02	0.264	19.02	1.86	90.2
0.04	0.176	19.02	1.30	93.2
0.06	0.172	19.02	1.27	93.3
0.08	0.172	19.02	1.27	93.3
0.10	0.194	19.02	1.41	92.6

APPENDIX C

Effect of Initial pH of CV dye solution on Percent Removal

pH	Initial absorbance (A)	Initial concentration (mg/L)	Final absorbance (A)	Final concentration (mg/L)	Percent dye removal (%)
2.09	3.052	19.7	0.346	2.4	87.8
4.30	2.856	18.4	0.190	1.4	92.4
6.00	2.660	17.2	0.202	1.5	91.3
9.20	2.616	16.9	0.206	1.5	91.1
10.70	1.676	10.9	0.260	1.8	83.5

APPENDIX D

Point of Zero Charge of BPP

Initial pH	Final pH	∆pH
1.99	2.24	0.25
4.00	5.01	1.01
6.05	5.06	-0.99
8.05	5.25	-2.80
9.95	5.19	-4.76

APPENDIX E

Effect of Initial Dye Concentration with Contact Time

Time taken (min)	C_0 = 4.7 mg/L		C_0 = 18.4 mg/L		C_0 = 35.0 mg/L	
	C_e (mg/L)	Percent removal (%)	C_e (mg/L)	Percent removal (%)	C_e (mg/L)	Percent removal (%)
2	0.7	85.1	3.0	83.7	5.2	85.1
4	0.7	85.1	2.6	85.7	4.1	88.3
6	0.6	87.2	2.3	87.5	3.7	89.4
8	0.6	87.2	2.2	88.0	3.5	90.0
10	0.5	89.4	1.9	89.7	3.4	90.3
15	0.5	89.4	1.8	90.2	2.5	92.9
20	0.5	89.4	1.5	91.8	2.5	92.9
25	0.6	87.2	1.3	92.9	2.4	93.1
30	0.7	85.1	1.3	92.9	2.1	94.0
45	0.6	87.2	1.2	93.5	2.0	94.3
60	0.6	87.2	1.2	93.5	1.7	95.1
120	0.5	89.4	1.2	93.5	1.7	95.1
180	0.6	87.2	1.3	92.9	1.6	95.4
240	0.7	85.1	1.1	94.0	1.5	95.7